Sinninghe Damsté et al. (2014) *Geochim. Cosmochim. Acta* **133**, 402-421

C_{27}-C_{30} Neohop-13(18)-enes and their saturated and aromatic derivatives in sediments: Indicators for diagenesis and water column stratification

Jaap S. Sinninghe Damsté [a,b*], Stefan Schouten [a,b], John K. Volkman [c]

[a] *NIOZ Royal Netherlands Institute for Sea Research, Department of Marine Organic Biogeochemistry, P.O. Box 59, 1790 AB Den Burg, The Netherlands.*
[b] *Utrecht University, Department of Geosciences, PO Box 80.021, Utrecht, The Netherlands.*
[c] *Sinopec Key Laboratory of Petroleum Accumulation Mechanisms, Wuxi Institute of Petroleum Geology, SINOPEC Research Institute of Petroleum Exploration and Production, 2060 Lihu Road, Binhu District, Wuxi, Jiangsu, 214126 China.*

As published in: *Geochim. Cosmochim. Acta* 133, 402-421 (2014)

Abstract

A limited suite of C_{27}, C_{29} and C_{30} rearranged hopenes identified as neohop-13(18)-enes have been reported in immature Recent and ancient marine/lacustrine sediments and their presence has been explained by dehydration and isomerisation of ubiquitous hopanols or hopenes. Here we investigated the source and fate of neohop-13(18)-enes in a range of recent and ancient sediments. The analysis of $\delta^{13}C$ values of hop-17(21)-ene and neohop-13(18)-ene in Arabian Sea surface sediments, in the Monterey Formation and in immature Cenomanian black shales show that they differ by 2-3‰, suggesting that the C_{30} neohop-13(18)-ene has a source different from those of the non-rearranged C_{30} hopenes. A new member of the family of neohop-13(18)-enes, the C_{28} hopene 28,30-dinorhop-13(18)-ene, was identified based on comparison of its mass spectral data with that of other members of the family of neohopenes. Its occurrence explains the formation of a series of orphan aromatic hopanoids bearing an ethyl group at C-21, known to occur in high concentrations in some organic-rich ancient sediments. Circumstantial evidence for this formation pathway is provided by identical $\delta^{13}C$ values for the C_{28} 28,30-dinorhop-13(18)-ene and two aromatic hopanoids in two Cretaceous black shales. Relatively abundant C_{28} 28,30-dinorhopene and related aromatic derivatives were present in ancient sediments where the distribution of other biomarkers (i.e. isorenieratene derivatives) indicated a stratified palaeo water column. Therefore, it is suggested that these compounds are derived from bacteria dwelling at or below the chemocline and may be used as indicators of stratified water bodies in the past. 28,30-Dinorhop-13(18)-ene may also be a precursor of the unusual C_{28} desmethylhopane 28,30-dinorhopane found in high concentrations in anoxic sediments and a limited suite of crude oils, which is consistent with the proposal that it too ultimately derives from bacteria living at the oxic-anoxic interface.

[*] Corresponding author. Tel. +31-222-369550; Fax: +31-222319674; *E-mail addresses*: damste@nioz.nl (J. Sinninghe Damsté), schouten@nioz.nl (S. Schouten), volkman.syky@sinopec.com (J.K. Volkman)

1. INTRODUCTION

Hopanoids occur ubiquitously in sediments and oils and are widely applied as biomarkers for bacteria. An important source for sedimentary hopanoids are the C_{35} bacteriohopanepolyol derivatives (Rohmer et al., 1980), which upon diagenesis result in the formation of hopanols, hopanoic acids, hopenes and hopanes. Bacteriohopanepolyols occur in the membrane of aerobic bacteria such as cyanobacteria, and heterotrophic and methanotrophic bacteria (e.g., Talbot et al., 2008; Řezanka et al., 2010). 2-Methyl hopanoids seem to be characteristic for cyanobacteria (Summons et al., 1999) although other sources are now known (Doughty et al., 2009). In addition to the extended hopanoids like the bacteriohopanepolyols, some bacteria also produce hopanoids without an extended chain at C-22. These include the C_{30} hopanoids, diplopterol (hopan-22-ol) and diploptene (hop-22(29)-ene), which are biosynthesized by quite a number of bacterial species (Rohmer et al., 1980). Hopanoids predominantly occur in aerobic bacteria in oxic environments and have only rarely have been found in facultatively anaerobic bacteria. However, in the last decade various anaerobic bacteria have also been shown to contain a range of hopanoid lipids including hop-22(29)-ene and hop-21-ene (Sinninghe Damsté et al., 2004; Fischer et al., 2005; Hartner et al., 2005).

The neohop-13(18)-enes are part of a special group of hopanoids; the so-called rearranged hopanoids (Moldowan et al., 1991; Farrimond and Telnaes, 1996). The carbon skeleton of these components is identical to that of the hopanes except that the methyl group normally at position C-18 is at position C-17. The presence of C_{30} (**I**; see Appendix for structures), and demethylated C_{29} (**II**) and C_{27} (**III**) neohop-13(18)-enes in Recent and ancient marine and lacustrine sediments has been noted for many years (e.g. Brassell and Farrimond, 1986; Comet et al., 1981; McEvoy et al., 1981; Thompson et al., 1982; Stein et al., 1988; Rullkötter et al., 1984; van Kaam-Peters et al., 1997, 1998; van Dongen et al., 2006a,b). It has been proposed that these components have been formed from ubiquitous hopanols or hopenes through dehydration and isomerisation reactions.

Here we examine the distribution of these compounds in a range of sediments and use $\delta^{13}C$ data to examine their likely origins. We show that a direct biological production of some neohopenes is likely and that a novel C_{28} dinorhop-13(18)-ene (**IV**) is the precursor of a well-known series of orphan aromatic hopanoids **(V-VIII**) and probably of 28,30-dinorhopane.

2. EXPERIMENTAL

2.1. Sample material

Sediments from a wide variety of sources were used in this study. These include Holocene sediments from the Arabian Sea, Miocene sediments from the Monterey Formation (USA), Maastrichtian black shales from the Ghareb Formation (Jordan), Cenomanian/Turonian black shales from the proto North Atlantic Ocean, and sediments from the Jurassic Kimmeridge Clay Formation (UK). Details on sampling and sediment characteristics have been described in other published studies (see Tables 1-3).

2.2. Extraction and fractionation

Typically, powdered samples (15 to 30 g) were Soxhlet extracted with dichloromethane (DCM)/methanol (7.5:1, v/v) for 24 h. An aliquot (ca. 250 mg) of the extract to which a mixture of four standards was added for quantitative analyses (Kohnen et al., 1990), was separated into an apolar and a polar fraction using a column (20 x 2 cm) packed with alumina (activated for 2.5 h at 150 °C) by elution

with hexane/DCM (9:1, v/v; 150 ml) and methanol/DCM (1:1, v/v; 150 ml), respectively. When visible amounts of elemental sulfur were present, activated (i.e. pretreated with 6 M HCl) copper powder was added to the apolar fractions dissolved in DCM and the resulting slurries were stirred for 12 h at room temperature to remove elemental sulfur. Apolar fractions (ca. 10 mg) were further separated by argentation thin layer chromatography (TLC) as described in Kohnen et al. (1990). Four to six fractions were scraped off the TLC plate and extracted with ethyl acetate using ultrasonication (x3). For measurement of the $\delta^{13}C$ values of hopenes, the most apolar TLC fractions were further separated where appropriate.

2.3. Analytical methods

Gas chromatographic (GC) analyses were performed using a Hewlett-Packard 5890 instrument, equipped with an on-column injector and a flame ionization detector. A fused silica capillary column (25 m x 0.32 mm) coated with CP-Sil 5 (film thickness 0.12 μm) was used with helium as carrier gas. The samples were dissolved in ethyl acetate and injected at 70 °C. Subsequently the oven was programmed to 130 °C at 20 °C/min and then at 4 °C/min to 320 °C where the temperature was maintained for 20 min. GC-MS was performed using a Hewlett-Packard 5890 gas chromatograph interfaced to a VG Autospec Ultima Q mass spectrometer operated at 70 eV with a mass range *m/z* 50-800 and a cycle time of 1.8 s (resolution 1000). The column conditions and temperature program were the same as described above for GC analyses. Concentrations for hop-13(18)-enes were determined by integration of mass chromatograms of *m/z* 176, 190, 204, and 218 for the C_{27}-C_{30} neohop-13(18)-enes, respectively, and *m/z* 83 for the internal standard. Response factors were determined by analyzing fractions containing neohopenes in high abundance co-injected with the mixture of standards and quantifying the appropriate peak areas in both the FID chromatogram and the specific mass chromatograms. The aromatic hopanes were determined by integration of mass chromatograms *m/z* 364, 346, and 328 for the mono-, di-, and triaromatic hopanoids, respectively, and *m/z* 107+147 for the internal standard using response factors for the different components. The presence of 17α,18α,21β(H)-dinorhopane was established by a positive co-injection experiment on two different stationary GC phases using an authentic standard (Chiron).

Compound-specific $\delta^{13}C$ analyses were performed using a Finnigan Delta C isotope ratio monitoring-gas chromatography-mass spectrometry (irm-GC-MS) system. A Hewlett-Packard 5890 gas chromatograph was used with the same column conditions and temperature program as described above for GC analyses. The $\delta^{13}C$ values for individual compounds are reported in the standard delta notation against the VPDB standard and are the means of duplicate runs with a reproducibility of typically <0.5‰ unless otherwise specified. The biomarkers for which $\delta^{13}C$ values are reported were sufficiently resolved by GC to be analysed by irm-GC/MS.

3. RESULTS

3.1. Occurrence of neohop-13(18)-enes

The distribution of neohop-13(18)-enes was determined in a large suite of sediments ranging in age from Recent to Jurassic (Tables 1-3). These compounds were identified on basis of their characteristic mass spectra (Fig. 1) and relative retention time data in comparison with those of authentic standards and literature data (e.g., Howard et al., 1984; Ageta et al., 1987; Douka et al., 2001). In all cases where neohopenes were encountered the C_{30} neo-13(18)-hopene (**I**) is present, sometimes together with the C_{29} member (**II**), in other cases with the C_{27} member (**III**), and sometimes with both (Tables 1-3). The C_{28} member of this series was not observed in any of these sediments nor did we find any

examples of neohop-13(18)-enes having more than 30 carbon atoms. Typical distributions in Holocene and Cretaceous sediments are shown in Figs. 2 and 3, respectively.

A new member of the family of neohop-13(18)-enes, 28,30-dinorhop-13(18)-ene (**IV**), was identified in Cenomanian (93.5 Ma old) black shales from the proto North Atlantic Ocean (Table 1) and in the Miocene Monterey Formation (Table 2). Its identification is based on comparison of its mass spectral data with those of the other members of the family (Fig. 1). The characteristic fragment ions containing the DE-ring part of 28,30-dinorhop-13(18)-ene (Table 4) are all shifted 14 Da to higher *m/z* values relative to those of the C_{27} neohop-13(18)-ene and 14 Da to lower *m/z* values relative to those of the C_{29} neohop-13(18)-ene. The $M^{+\bullet}$-29 fragment ion (Fig. 1b) indicates that the C_{28} 28,30-dinorhopene contains an ethyl group like the C_{29} neohopene. This indicates that, in comparison with the C_{29} neohopene, the C_{28} hop-13(18)-ene is missing either the C-27 or the C-28 methyl group. Loss of C-27 would, however, significantly affect the mass spectral fragmentation through ring C, the most important mass spectral fragmentation pathway of the neohopenes (Table 4). Therefore, the C_{28} neohopene is identified as 28,30-dinorhop-13(18)-ene (**IV**). Its exact stereochemical configuration (i.e. at C-17 and C-21), however, remains undetermined. Note that this neohopene is formally not a rearranged hopanoid since it does not bear a methyl group at C-17.

The C_{28} 28,30-dinorhopene is sometimes the most abundant neohopene: e.g., in some Cenomanian black shales deposited in the southern part of the proto North Atlantic Ocean (Fig. 3; Table 1). In other sediments the C_{28} hop-13(18)-ene cannot be detected (Table 1-3; Fig. 2), even though other hop-13(18)-enes are present, implying that there are specific environmental features and/or a specific source related to the occurrence of this compound. In the studied section of the Santa Barbara-Ventura Basin (Table 2) it occurs in some (but not all) rocks of the Miocene Monterey Formation but not in the underlying Rincon Shale and overlying Sisquoc Formation.

To determine potential diagenetic relationships the $\delta^{13}C$ values of the series of neohop-17(21)-enes and hop-17(21)-ene (**IX**) were measured for a selection of sediments and are reported in Table 5. Hopenes often elute in complex clusters of biomarkers (e.g., see the mass chromatograms of *m/z* 191 in Figs. 2 and 3), which hampers accurate determination of $\delta^{13}C$ values. Therefore, fractionation of apolar fractions of the extracts by preparative TLC and other clean-up techniques were required to obtain the values reported in Table 5. Values range from -16 to -27‰.

3.2. Occurrence of aromatic hopanes

A series of potentially related aromatic hopanoids (**V**-**VII**) previously identified by Greiner et al. (1976, 1977), all containing an ethyl side chain, were detected in relatively high concentrations in the same sediments that were analyzed for neohopenes (Tables 1-3), except for the two Holocene Arabian Sea sediments. These components are sometimes the most abundant peaks in the total ion chromatograms of aromatic hydrocarbon fractions (e.g. Fig. 4). The tetra-aromatic hopanoid **VIII** **(**Greiner et al., 1976, 1977) was not detected in these fractions. To determine potential diagenetic relationships, the $\delta^{13}C$ values of the series of aromatic hopanes were measured for a selection of sediments and are reported in Table 5. Values range from -16 to -26‰.

The concentration of the aromatic hopanoids was also quantified in artificially matured sediments of the Maastrichtian Ghareb Formation using hydrous pyrolysis at temperatures in the range 200-300°C for three days (Table 6). This revealed an increase in concentration of almost an order of magnitude at 200°C, whilst concentrations started to decrease at temperatures >260°C. The triaromatic hopanoid (**VII**) becomes relatively more abundant at higher temperatures.

3.3. Occurrence of 28,30-dinorhopane

Concentrations and $\delta^{13}C$ values of 28,30-dinorhopane (DNH) were previously reported for sediments of the Monterey Formation (Schouten et al., 2002a,c). Here we report the concentration of 17α,18α,21β(H)-28,30-DNH (**X**) and $\delta^{13}C$ values for Cenomanian/Turonian black shales from the Tarfaya coastal basin. DNH was detected in sometimes high concentrations (up to 400 μg.g C_{org}^{-1}; Table 7) in the sediments deposited during Oceanic Anoxic Event-2 (OAE-2) and younger ones but not before OAE-2. The $\delta^{13}C$ value of DNH varies from –22 to –28 ‰ (Table 7).

4. DISCUSSION

4.1. Biological sources of neohopenes

Neohopenes have been reported in a small number of microbes and ferns. Bottari et al. (1972) in their review of hydrocarbons in ferns noted that a few contain small amounts of neohop-13(18)-ene in addition to a range of hopenes and fernenes. In bacteria, neohop-13(18)-ene has been reported as a trace constituent of *Alicyclobacillus acidocaldarius* (Ageta et al., 1994) and in the purple non-sulfur bacterium *Rhodomicrobium vannielii* together with hop-17(21)-ene (**IX**), fern-7-ene and fern-9(11)-ene (Howard et al., 1984). Hop-17(21)-ene, neohop-13(18)-ene and diploptene (**XI**) have been found as trace constituents of *Frankia* sp. (Rosa-Putra, 1998). Douka et al. (2001) identified neohop-13(18)-ene together with hop-17(21)-ene, neohop-12-ene, fern-8-ene, diploptene and hop-21-ene (**IX**) in the bacterium *Zymonas mobilis*. There is no example thus far where the abundance of neohop-13(18)-ene is particularly high relative to other hopenes and so a direct contribution from bacteria cannot account for the high amounts of neohop-13(18)-ene found in some sediments. Moreover, there appear to be no reports of bacteria containing neohop-13(18)-enes having other than a C_{30} carbon number so the C_{27} and C_{29} neohop-13(18)- enes must be produced in the sediment. It is also unlikely that all members of the neohopene series could have the same origin since their $\delta^{13}C$ values differ by up to 6‰ in the sediments examined here (Table 5).

4.2. Possible formation of neohopenes through isomerisation of hopanoids

It has been proposed that neohopenes are formed from ubiquitous hopanols or hopenes through dehydration and isomerisation reactions (e.g., Moldowan et al., 1991). Ageta et al. (1987) reported that neohop-12-ene was readily converted to neohop-13(18)-ene by mild acid and that the conversion could also occur on alumina. Moreover, neohop-13(18)-ene (**I**) is formed when hopenes are isomerised under strong acidic conditions (Berti and Bottari, 1968). Ensminger (1977) also reported the formation of neohop-13(18)-ene (**I**) from refluxing diploptene (hop-22(29)-ene; **XI**) in the presence of the clay mineral montmorillonite for one hour, although at room temperature only hop-17(21)-ene (**IX**) and hop-21-ene (**XII**) were formed after 7 days. This suggests that the isomerisation of diploptene to hop-17(21)-ene is relatively facile, but that harsher reaction conditions or longer times are required for the subsequent isomerisation to neohop-13(18)-ene (Fig. 5). Note, however, that Moldowan et al. (1991) added diploptene to dried montmorillonite and after agitation for just 1 h at 25 °C the diploptene was completely converted to hop-l7(21)-ene and 17α-methyl-28-norhop-13(18)-ene (i.e. neohop-13(18)-ene) in a 3:1 ratio. These data also show that C_{27}-C_{29} neohopenes may be formed by isomerisation of other C_{27}-C_{29} hopenes in sediments, which is plausible since such components have been reported (e.g., 22,29,30 trisnorhop-17(21)-ene; Thompson et al., 1982), although they are much less common than the C_{30} hopanoids.

One way to test a possible formation of neohopenes from isomerisation of hopanoids is to compare their carbon isotopic compositions since $\delta^{13}C$ values of biomarkers are not likely to change during diagenetic reactions such as isomerisation and aromatisation (e.g., Freeman et al., 1990; Koopmans et al., 1996; Sinninghe Damsté et al., 1999). Therefore, the $\delta^{13}C$ values of hop-17(21)-ene (**IX)** and its inferred isomerisation product neohop-13(18)-ene (**I**) were determined in sediments where both components co-occur (Table 5). In a Recent Arabian Sea surface sediment from within its oxygen-minimum zone the $\delta^{13}C$ values of hop-17(21)-ene and neohop-13(18)-ene differ by 3.5‰. In a sediment from the Miocene Monterey Formation they differ by 5.5‰. In an immature Cenomanian black shale the difference is relatively small: only 1.8‰. These data clearly indicate that in these sediments neohop-13(18)-ene cannot have been formed solely by isomerisation of hop-17(21)-ene (Fig. 5) and thus likely has a source different from those of non-rearranged C_{30} hopenes as also suggested by Farrimond and Telnaes (1996). However, Köster et al. (1998) reported distinct, depleted δ^{13}values (-43.5‰) for both hop-17(21)-ene and neohop-13(18)-ene in a black shale from the Oligocene Menilite Formation (Poland), suggesting that in this case there was a clear diagenetic relationship. Alternatively, both components in this specific case may have originated from one organism.

4.3. An independent source for C_{28} 28,30-dinorhop-13(18)-ene

Although neohop-13(18)-ene, and to a lesser extent, the C_{27} and C_{29} neohopenes, are fairly common (Tables 1-3; Fig. 2), the occurrence of the C_{28} 28,30-dinorhop-13(18)-ene is much more limited; it was detected only in some sediments of the Monterey Formation and Cretaceous black shales but it was not detected in the Kimmeridge Clay Formation (Tables 1-3). The $\delta^{13}C$ value of C_{28} hop-13(18)-ene in a black shale from the Cape Verde Basin (DSDP Site 367) differs by 6‰ from that of the C_{30} neohop-13(18)-ene (Table 5). This, together with its more limited occurrence, suggests that the C_{28} hop-13(18)-ene is derived from an independent specific biological source. C_{28} 28,30-dinorhop-13(18)-ene only occurs in sediments deposited in the southern part of the proto North Atlantic Ocean during the Cenomanian/Turonian Oceanic Anoxic Event-2 (OAE-2), but it is absent in black shales deposited outside this area (Fig. 6). This is exactly the area that was previously characterized by the occurrence of photic zone euxinia (i.e. the base of the photic zone was comprised of anoxic, sulfide-containing water) by the relatively high abundance of derivatives of isorenieratene, the characteristic carotenoid of photosynthetic and anoxygenic brown coloured green sulfur bacteria (Sinninghe Damsté and Köster, 1998). This implies that the occurrence of the C_{28} 28,30-dinorhop-13(18)-ene may be related to the strong stratification of the ocean at that time and one could speculate that it is produced by bacteria residing at the chemocline although it has, to the best of our knowledge, not yet been reported in present-day stratified systems, such as the Black Sea and the Cariaco Basin. Further circumstantial evidence for this hypothesis is obtained from biomarker analyses of the OAE-2 section of DSDP Site 367, right in the core of the area characterized by photic zone euxinia (Fig. 6). Sediments deposited at this abyssal site are organic-rich, i.e. with a TOC content often >10% with values as high as almost 40% (Fig. 7a). Previous analyses revealed substantial variations in the concentrations of sulfur-bound isorenieratene (Fig. 7b; Kuypers et al., 2002) and our current analyses reveal that the concentration profile of the C_{28} 28,30-dinorhop-13(18)-ene (Fig. 7c) shows some correspondence with that of sulfur-bound isorenieratene. This is consistent with an origin for the C_{28} 28,30-dinorhop-13(18)-ene from bacteria residing at the chemocline. Analyses of an OAE-2 section from Site 603B in the northern part of the proto North Atlantic revealed the absence of the C_{28} 28,30-dinorhop-13(18)-ene (Table 1), in line with the reported absence or relatively low abundance of isorenieratene derivatives in these black shales (Kuypers et al., 2004).

4.4. Aromatisation of C_{28} 28,30-dinorhop-13(18)-ene

The C_{28} 28,30-dinorhop-13(18)-ene **(IV)** is a possible precursor of a series of orphan aromatic hopanes bearing an ethyl group at C-21 (**V-VIII**). The C_{24} tetra-aromatic and C_{25} triaromatic members of this series were identified in relatively high concentrations in the Messel oil shale (Greiner et al., 1976, 1977) and have subsequently been found, together with the C_{26} diaromatic and C_{27} monoaromatic members (**V-VI**), in many other, often thermally immature, organic matter-rich sediments (e.g., Barnes et al., 1979; Comet et al., 1981; Simoneit, 1981; Rullkötter et al., 1984; van Kaam Peters et al., 1997; van Dongen et al., 2006a). Their structures suggest a diagenetic sequence of successive aromatization reactions from ring D through rings C, B, and A (Greiner et al., 1976, 1997) (Fig. 8). The presence of an ethyl side-chain in **V-VIII** and the absence of homologues possessing an isopropyl group were enigmatic at the time since this suggested an unknown 30-norhopanoid precursor (Greiner et al., 1976, 1977).

The C_{28} 28,30-dinorhopene **IV** identified here seems to be a logical precursor of aromatic hopanoids **V-VIII** since it already possesses a double bond in ring-D and only one methyl group (C-27) has to be removed in the first aromatisation reaction leading to **V** (Fig. 8) in contrast to two methyl groups in the case of neohopenes **I-III**. Circumstantial evidence for this formation pathway comes from the tentative identification of the intermediate **XIII** in this reaction pathway (Fig. 8). The mass spectrum (Fig. 9) of this intermediate indicates that it is probably 28,30-dinorhop-13(18),16-diene. It is characterized by a molecular ion at *m/z* 380, 2 Dalton less than that of the C_{28} 28,30-dinorhopene (Fig. 1b), and a large $M^{+\bullet}$-29 fragment ion. The relatively high abundance of this latter fragment ion suggests that the additional unsaturation is a 16(17)-double bond, which facilitates the loss of the ethyl side-chain through β-cleavage. This component was identified in an extract of a Cenomanian black shale from the Demarara Rise (DSDP Site 144). This black shale also contains its presumed precursor and products, the C_{28} 28,30-dinorhopene **IV** (Table 1) and the aromatic hopanoids **V-VII** (Fig. 3).

More direct evidence for the proposed precursor-product relationship comes from the identical $\delta^{13}C$ values of the aromatic hopanoids **V** and **VI** and their proposed precursor **IV** in two immature Cenomanian black shales (Table 5). In the black shale from the Demarara Rise all three components have $\delta^{13}C$ values of ca. –26‰, whereas in the black shale from the Cape Verde Basin these values are also identical (ca. –15.5‰; Table 5). It seems that only the C_{28} 28,30-dinorhopene acts as a precursor of **V-VII,** since in the set of thermally immature OAE-2 black shales only the sediments containing the C_{28} 28,30-dinorhopene **IV** also contain the aromatic hopanoids **V-VII** in substantial amounts (Fig. 6). The relationship between **IV** and the aromatic hopanoids is also evident from the OAE-2 section from DSDP Site 367 (Fig. 7), although sediments that do not contain **IV** still contain relatively low, and sometimes even higher, concentrations of the aromatic hopanoids. This latter observation is most evident for the sediments of the S13 borehole in Morocco; they do contain substantial amounts of isorenieratene derivatives and aromatic hopanoids but the C_{28} 28,30-dinorhopene **IV** is absent (Table 1; Fig. 6). This may be due to the higher level of thermal maturity (i.e. the ββ hopane isomerisation index is 0.15, whereas for most OAE-2 black shales it is ~0.7; Table 1); it is expected that the C_{28} 28,30-dinorhopene **IV** is rapidly converted into aromatic hopanoids **V-VII**, whereas neohopenes **I-III** remain unaffected. This is also seen for the two black shales from DSDP Site 368. These sediments are affected by a diabase intrusion (Simoneit et al., 1981). The sediment at 952.65 mbsf was apparently not affected by the diabase sill (ββ hopane isomerisation index of 0.85) and has a neohopene distribution similar to that of other black shales in this area (Fig. 6), whereas the sediment at 979.20 mbsf was clearly affected by the diabase sill (ββ hopane isomerisation index of 0.00) and does not contain **IV** but contains substantial amounts of the aromatic hopanoids **VI** and **VII**.

The rapid conversion of the C_{28} 28,30-dinorhopene **IV** into aromatic hopanoids **V-VII** is consistent with the composition of the thermally more mature sediments of the Jurassic Kimmeridge Clay Formation. They do contain the C_{29} and C_{30} neohopenes **I** and **II** but not **IV**, which, in combination with sometimes high abundances of the aromatic hopanoids **V-VII** (Table 3; Fig. 4b), suggests a complete conversion of **IV**. In a section of the Kimmeridge Blackstone Band, a ca. 1 m thick interval reaching C_{org} levels of over 40% (Fig. 10a), the concentration of the aromatic hopanoids (normalized on C_{org}) clearly maximizes in this interval (Fig. 10c). This is consistent with the idea that the C_{28} 28,30-dinorhopene **IV** and, thus, its diagenetic derivatives **V-VII**, can be used as stratification markers since it is well established that the Blackstone Band was deposited in a stratified, euxinic shelf sea (van Kaam-Peters et al., 1997, 1998; van Dongen et al., 2006a) as is also evident from increased levels of isorenieratene derivatives (Fig. 10b). With the assumption that the C_{28} 28,30-dinorhopene **IV** is quantitatively converted into **VI** and**VII**, the original neohopene distribution can be calculated; the C_{28} 28,30-dinorhopene clearly shows the highest abundance in the Blackstone Band (Fig. 10d).

An intriguing observation remains that the concentrations of the aromatic hopanoids **V-VII** are almost always substantially higher than that of C_{28} 28,30-dinorhopene **IV** (Tables 1-3); quantitative conversion would be expected to give rise to concentrations never exceeding ca. 30 μg.g C_{org}^{-1} (highest concentration measured), whereas the concentration of the aromatic hopanoids **V-VII** is often substantially higher, especially in thermally more mature sediments (Tables 1-3). This suggests some kind of sequestration of the C_{28} hopane skeleton in high-molecular-weight fractions (e.g. kerogen). This is confirmed by mild artificial maturation experiments (hydrous pyrolysis at temperatures of 200-300°C) of an organic-rich limestone from the Upper Cretaceous Ghareb Formation (Koopmans et al., 1998). Heating at 200°C for 72 h resulted in a seven-fold increase in the concentration of the aromatic hopanoids **V-VII** (Table 6). At higher temperatures the concentration remained more or less constant with a substantial decrease at 280°C and higher (Table 6). Whether this is due to conversion into **VIII** is not clear since this tetra-aromatic hopanoid was not detected in the apolar fractions studied. These artificial maturation experiments also suggest that the degree of aromatization increases with increasing level of thermal maturity (Table 6), in line with the proposed reaction pathway (Fig. 8). In general this is also consistent with the data on the natural sediments; the immature OAE-1 black shales contain a relatively high abundance of the monoaromatic hopanoid **V** (Table 1), whereas the more thermally mature Jurassic Kimmeridge Clay sediments only contain the di- and triaromatic hopanoids **VI** and **VII** (Table 3). However, within specific sections (e.g. Fig. 7e) marked changes can be seen, clearly indicating that factors other than thermal maturity also affect the distribution of the aromatic hopanoids.

4.5. Conversion of neohopenes to hopanes

The presence of rearranged hopanes in crude oils has been known for many years and it has been established that they are more stable than non-rearranged hopanes (Moldowan et al., 1991). It is generally accepted that they are formed from unrearranged hopanoid natural products through chemical mechanisms during diagenesis (Moldowan et al., 1991). For example, the C_{27} rearranged hopane 18α(H)-22,29,30-trisnorneohopane (Ts; **XIV**) is more stable than 17α(H)-22,29,30-trisnorneohopane (Tm; **XV**) giving rise to the widely used maturity parameter Ts/Tm. Hydrogenation of the double bond in C_{27} neohop-13(18)-ene readily affords Ts and this is consistent with the fact that environmental factors such as Eh and pH are also known to affect the Ts/Tm ratio (Moldowan et al., 1986). Similarly, the C_{29} norneohop-13(18)-ene is a logical precursor of the C_{29} pseudohomologue of Ts (i.e. 18α(H)-17α-methyl-28,30-DNH) which was nicknamed C_{29}Ts by Moldowan et al. (1991) who confirmed its structure. Of interest is that there have been no reports of the C_{30} pseudohomologue of the 18α(H)-neohopane series (Moldowan et al., 1991), while this could be potentially be produced from neohop-

13(18)-ene by reduction of the double bond.

Seifert et al. (1978) and Moldowan et al. (1984) identified three unusual $C_{28}H_{48}$-pentacyclic hopanes in Monterey shale as 17α,18α,21β(H)-28,30-bisnorhopane (**X**), 17β,18α,21β(H)-28,30-bisnorhopane, and 17β,18α,21α(H)-28,30-bisnorhopane using X-ray crystallography. Note that these compounds are now referred to as DNHs rather than bisnorhopanes. The epimer present in thermally immature sediments is 17α,18α,21β(H)-DNH, while the 17β,18α,21α(H) isomer is abundant in a limited suite of crude oils (e.g., Monterey oils; Peters et al., 2008). Schoell et al. (1992) demonstrated by compound specific isotope analysis that 17β,18α,21α(H)-28,30-DNH is a thermal product of 17α,18α,21β(H)-28,30-DNH.

Our identification of the C_{28} 28,30-dinorhopene **IV** raises the question if this hopene would be a plausible precursor of 17α,18α,21β(H)-DNH. The carbon skeleton is identical (both components are characterized by the uncommon ethyl substitution of the cyclopentane ring) and only hydrogenation of the double bond would be required to form this DNH from **IV**. However, we did not determine the exact stereochemistry of dinorneohopene **IV** and are, thus, unable to predict if hydrogenation of the 13,18-double bond would indeed result in formation of 17α,18α,21β(H)-DNH, which has an unusual stereochemistry compared to most hopanoids present in immature black shales. To test a potential relationship their $\delta^{13}C$ values should be compared. Unfortunately, none of the studied sediments contained both components in sufficient amounts for $\delta^{13}C$ values to be measured with confidence. However, in the Miocene Monterey Formation, some sediments contained both DNH **XI**, and the related trinorhopane (which lacks a methyl at C-25), and the triaromatic hopanoid **VII** (likely derived from C_{28} dinorhopene). For sediment KG10, the $\delta^{13}C$ values of these compounds are identical (Table 5), supporting a relationship. However, for KG1, where DNH is anomalously depleted in ^{13}C (Fig. 11b), they are different (Table 5). However, when we compare the concentration profiles of DNH and the C_{28} dinorhopene for this section (Figs. 11c and d) a clear correspondence is observed, suggestive of a precursor-product relationship. The profile of the summed concentration of the aromatic hopanoids **V-VII** (Fig. 11e) shows a less clear correspondence to those of DNH and the C_{28} dinorhopene (cf. Figs. 11c and d). Perhaps this is caused by the fact that the C_{28} dinorhopene is converted into both DNH and the aromatic hopanoids **V-VII** and that under certain depositional conditions one of these two pathways may be favoured.

For the Cenomanian/Turonian black shales it was noted that in the southern part of the proto North Atlantic Ocean characterized by strong anoxic conditions only the sediments of the Tarfaya Basin did not contain the C_{28} 28,30-dinorhopene (Fig. 6). Remarkably, however, these sediments do contain relatively high amounts of 17α,18α,21β(H)-DNH (Fig. 12c), suggesting that their higher level of thermal maturity (Table 1) has resulted in complete conversion of the C_{28} dinorhopene into DNH and aromatic hopanoids **V-VII**. Comparison of the DNH concentration profile with that of isorenieratene derivatives again shows a good correspondence, suggestive that the precursor of DNH is associated with anoxic conditions (cf. Figs. 12c and 12d). The $\delta^{13}C$ record of DNH (Fig. 12b) shows quite some variation. However, most of this variation is also observed for algal-derived steranes and C_{org} in general (Fig. 12b) and is related to the positive isotope excursion associated with OAE-2 (Kuypers et al., 2002; Sinninghe Damsté et al., 2008). In comparison with the Monterey Formation (Fig. 11b) DNH in the Tarfaya Basin is more enriched and is even more enriched in ^{13}C than $C_{org.}$

Several authors have associated the presence of C_{28} DNH in sediments and oils with production by anaerobic bacteria in an anoxic depositional environment (e.g., Grantham et al., 1980; Katz and Elrod, 1982; Mello et al., 1988, 1989; Schoell et al., 1992; Nytoft et al., 2000). High contents of the C_{28} DNH

occur in pelagic carbonates deposited in the Lower Cambrian Sinyaya Formation together with smaller amounts of the C_{27}-C_{32} homologues (Parfenova et al., 2010). Peters et al. (2008) attributed the presence of 28,30-DNH in Monterey oils to suboxic to anoxic marine conditions during source rock deposition. Schoell et al. (1992) showed from $\delta^{13}C$ data that all three 28,30-DNH isomers in a Monterey crude oil must have the same source, which is different from the extended hopanes and postulated that they were derived from chemoautotrophic bacteria living at the oxic/anoxic layer in the water columns and sediments. Since the DNHs only occurred in the free hydrocarbon fraction, they suggested that any functional group in the precursor lipid must be shielded and thus proposed either 28,30-dinorhop-17-ene or 28,30-dinorhop-13(18)-ene (**IV**) as possible candidates. Schouten et al. (2000a) showed for an outcrop section at Naples Beach (USA) that the laminated sediments from the Monterey Formation contained high abundances of 28,30-DNH (and 25,28,30-trinorhopane), but that the more oxic sediments of the underlying Rincon Shale and overlying Sisquoc Formation contained only traces of these components (Fig. 11c). A high resolution study of sediments of the Monterey Formation from a core from the Santa Maria Basin showed that the relative abundance of DNH on a meter scale is highly variable (Curiale and Odermatt, 1989). This is consistent with our data of the Tarfaya Basin (Fig. 12c), which also shows a large variation in concentration, probably depending on specific conditions in the (anoxic) depositional environment.

These data and those reported here support the contention that the C_{28} 28,30-dinorhop-13(18)-ene and 28,30-DNH might both be derived from a functionalized C_{28} hopanoid associated with bacteria that thrive at the oxic/anoxic boundary in low-oxygen, marine depositional environments. The $\delta^{13}C$ values varied over a considerable range (-21 to -31 ‰), whereas those of other biomarkers were less variable (Fig. 11b; Schouten et al., 2000c). The observed high variability in $\delta^{13}C$ values of DNH (e.g. Schoell et al., 1992; Köster et al., 1998; Schouten et al., 1997, 2000c; Figs. 11b and 12b) and 28,30-dinorhop-13(18)-ene and its aromatic derivatives (Table 4) would be consistent with a niche at the chemocline since there is a steep gradient in $\delta^{13}C$ of dissolved inorganic carbon at chemoclines (e.g., van Breugel et al., 2006), which likely results in carbon isotope variability in the lipids of (chemo)autotrophic bacteria residing at the chemocline.

5. CONCLUSIONS

C_{27}-C_{30} hopenes having a double bond at 13(18) (neohop-13(18)-enes) are present in a number of thermally immature sediments and seem to be most abundant in sediments where clay-catalyzed double bond isomerisation occurs. A plausible sequence of transformations from hop-22(29)-ene to hop-21-ene to hop-17(21)-ene to neohop-13(18)-ene can be envisaged but differences in the $\delta^{13}C$ values suggests that this cannot explain the distributions in all sediments and that other sources must be involved. Relatively abundant C_{28} 28,30-dinorhopene and related aromatised counterparts **V-VII** are present in a few sediments where the distribution of other biomarkers (e.g., isorenieratene derivatives) indicates a stratified palaeowater column. Therefore, it is suggested that the C_{28} 28,30-dinorhopene is derived from lipids of bacteria dwelling at or below the chemocline and may be used as an indicator of stratified water bodies in the past and by extension, its diagenetic product, the C_{28} 28,30-DNH, is also an indicator of these conditions.

ACKNOWLEGEMENTS

We thank DSDP/ODP for samples, Dr. P. Schaeffer and Dr. P. Albrecht for authentic standards of aromatic hopanoids, Dr. T. M. Peakman for an authentic neo-13(18)-ene standard, and present and former members of the BGC laboratory for laboratory assistance. We specifically thank Dr. M.M.M. Kuypers for his analytical work on OAE-2 black shales.

REFERENCES

Ageta H., Shiojima K. and Arai Y. (1987) Acid-induced rearrangement of triterpenoid hydrocarbons belonging to the hopane and migrated hopane series. *Chem. Pharm. Bull.* **35**, 2705-2716.

Ageta H., Shiojima K., Arai Y., Suzuki H. and Kiyotani T. (1994) NMR-spectra of triterpenoids. 2. Hopenes and migrated hopenes. *Chem. Pharm. Bull.* **42**, 39-44.

Barnes P. J., Brassell S. C., Comet P., Eglinton G., McEvoy J., Maxwell J. R., Wardroper A. M. K. and Volkman J. K. (1979) Preliminary lipid analysis of core sections 18, 24, and 30 from Hole 402A. In *Initial Reports of the Deep Sea Drilling Project*, vol. 48, US Government Printing Office, Washington, pp. 965-975.

Berti G. and Bottari F. (1968) Constituents of ferns. In *Progress in Phytochemistry* (eds L. Reinhold and V. Lipschitz), Vol. 1, Interscience, New York, pp. 589-685.

Bottari F., Marsili A., Morelli I. and Pacchiani M. (1972) Aliphatic and triterpenoid hydrocarbons from ferns. *Phytochemistry* **11**, 2519-2523.

Brassell S. C. and Farrimond P. (1986) Fluctuations in biological marker composition within a Cenomanian black shale from the Angola Basin. *Mitt. Geol. Paläontol. Inst. Univ. Hamburg* **60**, 311-338.

Comet P. A., McEvoy J., Brassell S. C., Eglinton G., Maxwell J. R. and Thomson I. D. (1981) Lipids of an Upper Albian limestone, Deep Sea Drilling Project Site 465, Section 465A-38-3. In *Initial Reports of the Deep Sea Drilling Project*, vol. 62, US Government Printing Office, Washington, pp. 923-937.

Cox B.M and Gallois R.W. (1981) The stratigraphy of the Kimmeridge Clay of the Dorset type area and its correlation with some other Kimmeridgian sequences. *Rep. Inst. Geol. Sci.* **80**, 1-44.

Curiale J. A. and Odermatt J. R. (1989) Short-term biomarker variability in the Monterey Formation, Santa Maria Basin. *Org. Geochem.* **14**, 1-13.

Doughty D. M., Hunter R. C., Summons R. E. and Newman D. K. (2009) 2-Methylhopanoids are maximally produced in akinetes of *Nostoc punctiforme*. Geobiological implications. *Geobiology* **7**, 524-532.

Douka E., Koukkou A. I., Drainas C., Grosdemange-Billiard C. and Rohmer M. (2001) Structural diversity of the triterpenic hydrocarbons from the bacterium *Zymomonas mobilis*: the signature of defective squalene cyclization by the squalene/hopene cyclase. *FEMS Microbiol. Lett.* **199**, 247-251.

Ensminger A. (1977) *Evolution de composés polycyclic sédimentaires*. Thèse de Doctorat ès Sciences, Universite Louis Pasteur, Strasbourg.

Farrimond P. and Telnaes N. (1996) Three series of rarranged hopanes in Toarcian Sediments (northern Italy). *Org. Geochem.* **25**, 165-177.

Fischer W. W., Summons R. E. and Pearson A. (2005) Targeted genomic detection of biosynthetic pathways: anaerobic production of hopanoid biomarkers by a common sedimentary microbe. *Geobiology* **3**, 33-40.

Freeman K. H., Hayes J. M., Trendel J. M. and Albrecht P. (1990) Evidence from carbon isotope measurements for diverse origins of sedimentary hydrocarbons. *Nature* **343**, 254-256.

Grantham P. J., Posthuma J. and de Groot K (1980) Variation and significance of the C_{27} and C_{28} triterpane content of a North Sea core and various North Sea crude oils. In *Advances in Organic Geochemistry 1979* (Edited by Douglas A. G. and Maxwell J. R.), pp. 29-38. Pergamon, Oxford.

Greiner A. C., Spyckerelle C. and Albrecht P. (1976) Aromatic hydrocarbons from geological sources - I. New naturally occurring phenanthrene and chrysene derivatives. *Tetrahedron* **32**, 257-260.

Greiner A. C., Spyckerelle C., Albrecht P. and Ourisson G. (1977) Aromatic hydrocarbons from

geological sources. Part V. Mono- and di-aromatic hopane derivatives. *J. Chem. Res. (S)* **334,** 3829-3871.

Hartner T., Straub K. L. and Kannenberg E. (2005) Occurrence of hopanoid lipids in anaerobic *Geobacter* species. *FEMS Microbiol. Lett.* **243**, 59-64.

Howard D. L., Simoneit B. R. T. and Chapman D. J. (1984) Triterpenoids from lipids of *Rhodomicrobium vanniellii*. *Arch. Microbiol.* **137**, 200-204.

Isaacs C. M., Pollastro R. M., Barron J. A., Ingle J. C. Jr., Bukry D., Dunbar R. B. Keller M. A., Tomson J. H. and Lewan M. D. (2000) Molecular biogeochemistry of Monterey sediments (Naples Beach, USA). II: Carbon isotopic compositions of free and sulphur-bound carbon skeletons. In *The Monterey Formation: From Rock to Molecule* (eds. C. M. Isaacs and J. Rullkötter), Cooperative Monterey Organic Geochemical Project, Columbia University Press, pp. 373-392.

Katz B. J. and Elrod L. W. (1982) Organic geochemistry of DSDP Site 467, offshore California, Middle Miocene to Lower Pliocene strata. *Geochim. Cosmochim. Acta* **47**, 389-396.

Kohnen M. E. L., Sinninghe Damsté J. S., Rijpstra W. I. C. and de Leeuw J. W. (1990) Alkylthiophenes as sensitive indicators of palaeoenvironmental changes: A study of a Cretaceous oil shale from Jordan. In *Geochemistry of Sulphur in Fossil Fuels* (eds. W. M. Orr and C. M. White), ACS Symposium Series 429, American Chemical Society, Washington DC, pp. 444-485.

Koopmans M. P., Köster J., van Kaam-Peters H. M. E., Kenig F., Schouten S., Hartgers W. A., de Leeuw J. W. and Sinninghe Damsté J. S. (1996) Diagenetic and catagenetic products of isorenieratene: Molecular indicators for photic zone anoxia. *Geochim. Cosmochim. Acta* **60**, 4467-4496.

Koopmans M. P., Rijpstra W. I. C., de Leeuw J. W., Lewan M. D. and Sinninghe Damsté J. S. (1998) Artificial maturation of an immature sulphur- and organic matter-rich limestone from the Ghareb Formation, Jordan. *Org. Geochem.* **28**, 503-521.

Köster J., Rospondek M., Schouten S., Kotarba M., Zubrzycki A. and Sinninghe Damsté J. S. (1998) Biomarker geochemistry of a foreland basin: the Oligocene Menilite Formation in the Flysch Carpathians of Southeast Poland. *Org. Geochem.* **29**, 649-669.

Kuypers M. M. M., Pancost R. D., Nijenhuis I. A. and Sinninghe Damsté J. S. (2002) Enhanced productivity led to increased organic carbon burial in the euxinic North Atlantic basin during the late Cenomanian oceanic anoxic event. *Paleoceanography* **17**, 10.1029/2000PA000569.

Kuypers M. M. M., Lourens L., Rijpstra W. I. C., Pancost R. D., Nijenhuis I. A. and Sinninghe Damsté J. S. (2004) Orbital forcing of organic carbon burial in the proto-North Atlantic during Oceanic Anoxic Event 2. *Earth Planet. Sci. Lett.* **228**, 465-482.

Kuhnt W., Nederbragt A. J. and Leine L. (1997) Cyclicity of Cenomanian-Turonian organic-carbon-rich sediments in the Tarfaya Atlantic Coastal Basin (Morocco). *Cretaceous Res*. **18**, 587–601.

McEvoy J., Eglinton G. and Maxwell J. R. (1981) Preliminary lipid analyses of sediments from Sections 467-3-3 and 467-97-2. In *Initial Reports of the Deep Sea Drilling Project*, vol. 63. US Government Printing Office, Washington, pp. 763-774.

Mello M. R., Telnaes N., Gaglianone P.C., Chicarelli M. I., Brassell S. C. and Maxwell J. R. (1988) Organic geochemical characterisation of depositional palaeoenvironments of source rocks and oils in Brazilian marginal basins. *Org. Geochem.* **13**, 31–45.

Mello M. R., Koutsoukos E. A. M., Hart M. B., Brassell S. C. and Maxwell J. R. (1989) Late Cretaceous anoxic events in the Brazilian continental margin. *Org. Geochem.* **14**, 529–542.

Moldowan J. M., Seifert W. K., Arnold E. and Clardy J. (1984) Structure proof and significance of stereoisomeric 28,30-bisnorhopanes in petroleum source rocks. *Geochim. Cosmochim. Acta* **48**,

1651-1661.

Moldowan J. M., Sundararaman P. and Schoell M. (1986) Sensitivity of biomarker properties to depositional environment and/or source input in the Lower Toarcian of SW-Germany. In *Advances in Organic Geochemistry 1985* (eds. D. Leythaeuser and J. Rullkötter), Pergamon Press Ltd., Oxford, U.K., pp. 915-926.

Moldowan J. M., Fago F. J., Carlson R. M. K., Young D. C., Van Duyne G., Clardy J., Schoell M., Pillinger C. T. and Watt D. S. (1991) Rearranged hopanes in sediments and petroleum. *Geochim. Cosmochim. Acta* **55**, 3333-3353.

Morgans-Bell H. S., Coe A. L., Hesselbo S. P., Jenkyns H. C., Weedon G. P., Marshall J. E. A., Tyson R. V. and Williams C. J. (2001) Integrated stratigraphy of the Kimmeridge Clay Formation (Upper Jurassic) based on exposures and boreholes in south Dorset, UK. *Geol. Mag.* **138**, 511-539.

Nytoft H.P., Bojesen-Koefoed J.A. and Christiansen F.G. (2000) C_{26} and C_{28}-C_{34} 28-norhopanes in sediments and petroleum. *Org. Geochem.* **31**, 25-39.

Parfenova T. M., Pushkarev M. S. and Ivanova E. N. (2010) Hopanes and hopenes of the Lower Cambrian Sinyaya Formation (northern slope of the Aldan Anteclise). *Doklady Earth Sci.* **430**, 129-133.

Peters K. E., Hostettler F. D., Lorenson T. D. and Rosenbauer R. J. (2008) Families of Miocene Monterey crude oil, seep, and tarball samples, coastal California. *AAPG Bull.* **92**, 1131-1152.

Řezanka T., Siristova L., Melzoch K. and Sigler K. (2010) Hopanoids in bacteria and cyanobacteria - their role in cellular biochemistry and physiology, analysis and occurrence. *Mini-Rev. Org. Chem.* **7**, 300-313.

Rohmer M., Dastillung M. and Ourisson G. (1980) Hopanoids from C_{30} to C_{35} in recent muds - chemical markers for bacterial activity. *Naturwissenschaften* **67**, 456-458.

Rosa-Putra S. (1998) *Rôle du 1-désoxy-D-xylulose dans la biosythèse des hopanoïds bactériens*. PhD thesis. Universite Louis Pasteur, Strasbourg.

Rullkötter J., Mukhopadhyay P. K. and Welte D. R. (1984) Geochemistry and petrography of organic matter in sediments from Hole 530A, Angola Basin, and Hole 532, Walvis Ridge, Deep Sea Drilling Project. In *Initial Reports of the Deep Sea Drilling Project*, vol. 75, US Government Printing Office, Washington, pp. 1069-1087.

Schoell M., McCaffrey M. A., Fago F. J. and Moldowan J. M. (1992) Carbon isotopic compositions of 28,30-bisnorhopanes and other biological markers in a Monterey crude oil. *Geochim. Cosmochim. Acta* 56, 1391-1399.

Schouten S., Schoell M., Rijpstra W. I. C., Sinninghe Damsté J. S. and de Leeuw J. W. (1997) A molecular stable carbon isotope study of organic matter in immature Miocene Monterey sediments (Pismo Basin). *Geochim. Cosmochim. Acta* **61**, 2065-2082.

Schouten S., De Loureiro M. R. B., Sinninghe Damsté J. S. and de Leeuw J. W. (2000a) Molecular biogeochemistry of Monterey sediments (Naples Beach, USA). I: Distributions of hydrocarbons and organic sulphur compounds. In *The Monterey Formation: From Rock to Molecule* (eds. C. M. Isaacs and J. Rullkötter), Cooperative Monterey Organic Geochemical Project, Columbia University Press, pp. 150-174.

Schouten S., Hoefs M. J. L. and Sinninghe Damsté J. S. (2000b) A molecular and stable carbon isotopic study of lipids in Late Quaternary sediments from the Arabian Sea. *Org. Geochem.* **31**, 509-521.

Schouten S., Schoell M., Summons R. E., Sinninghe Damsté J. S. and de Leeuw J. W. (2000c) Molecular biogeochemistry of Monterey sediments (Naples Beach, USA). II: Carbon isotopic compositions of free and sulphur-bound carbon skeletons. In *The Monterey Formation: From Rock to Molecule* (eds. C. M. Isaacs and J. Rullkötter), Cooperative Monterey Organic

Geochemical Project, Columbia University Press, pp. 175-188.
Scotese C. R. and Golonka J. (1992) Paleogeographic Atlas, University of Texas, Arlington.
Seifert W. K., Moldowan J. M., Smith G. W. and Whitehead E. V. (1978) First proof of structure of a C_{28}-pentacyclic triterpane in petroleum. *Nature* **271**, 456-457.
Simoneit B. R. T. (1981) Organic geochemistry of Albian sediments from Hess Rise, Deep Sea Drilling Project Hole 466. In *Initial Reports of the Deep Sea Drilling Project*, vol. 62, US Government Printing Office, Washington, pp. 939-942.
Simoneit B. R. T., Brenner S., Peters K. E. and Kaplan I. R. (1981) Thermal alteration of Cretaceous black shale by diabase intrusions in the eastern Atlantic. 2. Effects on bitumen and kerogen. *Geochim. Cosmochim. Acta* **45**, 1581-1602.
Sinninghe Damsté J. S. and Köster J. (1998) A euxinic southern North Atlantic Ocean during the Cenomanian/Turonian oceanic anoxic event. *Earth Planet. Sci. Lett.* **158**, 165-173.
Sinninghe Damsté J. S., Köster J., Baas M., Ossebaar J., Dekker M., Pool W. and Geenevasen J. A. J. (1999) A sedimentary tetrahydrophenanthrene derivative of tetrahymanol. *Tet. Lett.* **40**, 3949-3952.
Sinninghe Damsté J. S., Rijpstra W. I. C., Schouten S., Fuerst J. A., Jetten M. S. M. and Strous M. (2004) The occurrence of hopanoids in planctomycetes: Implications for the sedimentary biomarker record. *Org. Geochem.* **35**, 561-566.
Sinninghe Damsté J. S., Kuypers M. M. M., Pancost R. D. and Schouten S. (2008) The carbon isotopic response of algae, (cyano)bacteria, archaea and higher plants on the late Cenomanian perturbation of the global carbon cycle: Insights from biomarkers in black shales from the Cape Verde Basin (DSDP Site 367). *Org. Geochem.* **39**, 1703-1718.
Stein R., Rullkötter J., Littke R., Schaefer R. G. and Welte D. R. (1988) Organofacies reconstruction and lipid geochemistry of sediments from the Galicia Margin, Northeast Atlantic (ODP Leg 103). *Proc. Ocean Drilling Proj., Sci. Res.* **103**, 567-585.
Summons R. E., Jahnke L. L., Hope J. M. and Logan G. A. (1999) 2-Methylhopanoids as biomarkers for cyanobacterial oxygenic photosynthesis. *Nature* **400**, 554-557.
Talbot H. M., Summons R. E., Jahnke L. L., Cockell C. S., Rohmer M. and Farrimond P. (2008) Cyanobacterial bacteriohopanepolyol signatures from cultures and natural environmental settings. *Org. Geochem.* **39**, 232-263.
Thompson I.D., Brassell S.C., Eglinton G. and Maxwell J.R., (1982) Preliminary lipid analysis of Sections 481-2-2. In *Initial Reports of the Deep Sea Drilling Project*, vol. 64, US Government Printing Office, Washington, pp. 913-919.
van Breugel Y., Schouten S., Paetzel M. and Sinninghe Damsté J.S. (2006) Seasonal variation in the stable carbon isotopic composition of algal lipids in a shallow anoxic fjord: evaluation of the effect of recycling of respired CO_2 on the $\delta^{13}C$ of organic matter. *Am. J. Sci*. **306**, 367-387.
van Dongen B. E., Schouten S. and Sinninghe Damsté J. S. (2006a) Preservation of carbohydrates through sulfurization in a Jurassic euxinic shelf sea: Examination of the Blackstone Band TOC-cycle in the Kimmeridge Clay Formation, UK. *Org. Geochem.* **37**, 1052-1073.
van Dongen B., Talbot H. M., Schouten S., Pearson P. N. and Pancost R. D. (2006b) Well preserved Palaeogene and Cretaceous biomarkers from the Kilwa area, Tanzania. *Org. Geochem.* **37**, 539-557.
van Kaam-Peters H. M. E., Schouten S., de Leeuw J. W. and Sinninghe Damsté J. S. (1997) A molecular and carbon isotope biogeochemical study of biomarkers and kerogen pyrolysates of the Kimmeridge Clay facies: Palaeoenvironmental implications. *Org. Geochem.* **27**, 399-422.
van Kaam-Peters H. M. E., Schouten S., Köster J. and Sinninghe Damsté J. S. (1998) Controls on the molecular and carbon isotopic composition of organic matter deposited in a Kimmeridgian euxinic

shelf sea: Evidence for preservation of carbohydrates through sulfurisation. *Geochim. Cosmochim. Acta* **62**, 3259-3283.

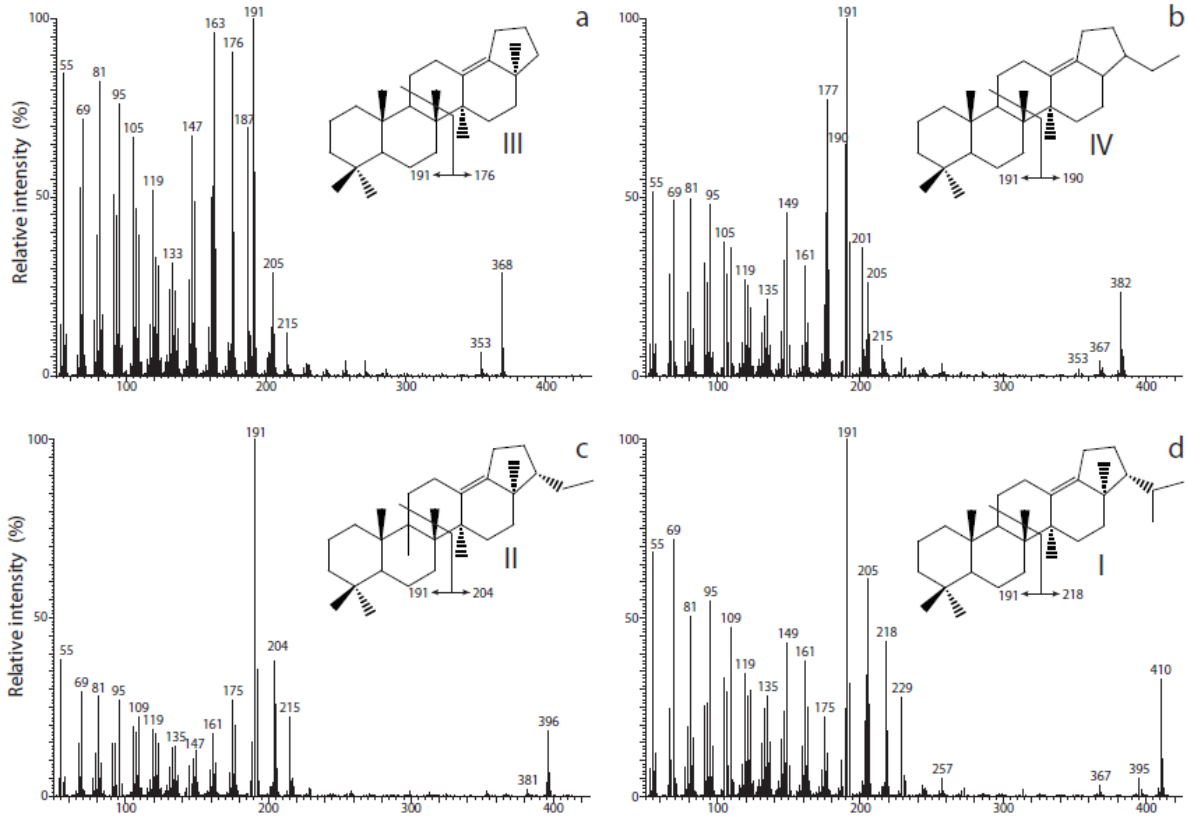

Fig. 1. Mass spectra (background subtracted) of (**a**) 22,29,30-trisnorneohop-13(18)-ene (**III**), (**b**) 28,30-dinorneohop-13(18)-ene (**IV**), (**c**) 30-norneohop-13(18)-ene (**II**), and (**d**) neohop-13(18)-ene (**I**). The characteristic fragmentation is indicated; further information is provided in Table 4.

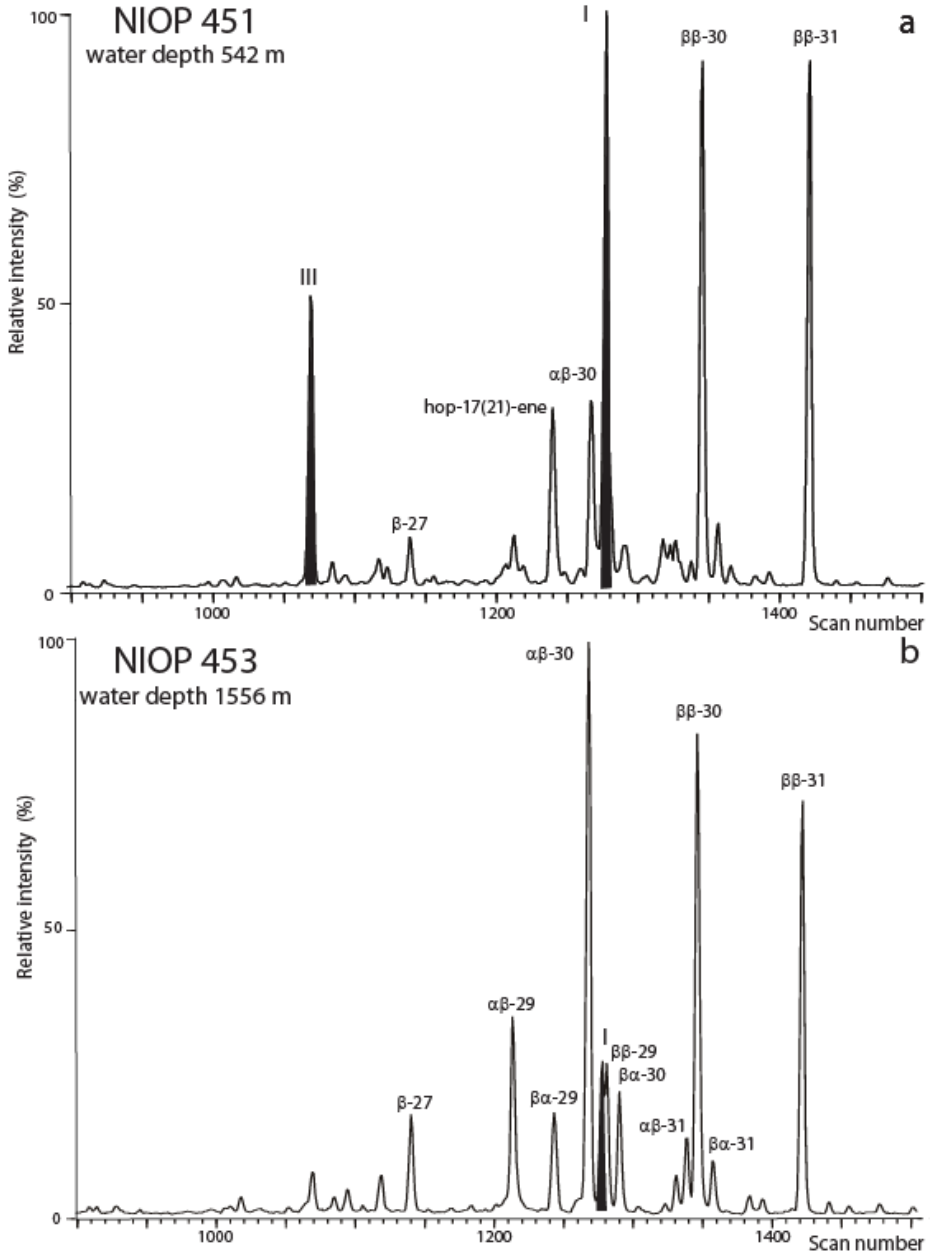

Fig. 2. Partial mass chromatograms of *m/z* 191 of the saturated hydrocarbon fraction (obtained by Ag^{+}-TLC) of extracts of sediments (0-100 cm) from (**a**) Netherlands Indian Ocean Program (NIOP) Site 451 (23 40'53'' N, 66 02'97'' E, water depth 542 m) and **(b**) NIOP Site 453 (23 15' 30'' N, 65 44'50'' E, water depth 1556 m). NIOP Site 451 and 453 are, respectively, within and below the oxygen minimum zone of the Arabian Sea. Peaks representing neo-13(18)-hopenes are black and hopanes are indicated by a shorthand notation indicating the stereochemistry at the C-17 and C-21 positions and total number of carbon atoms.

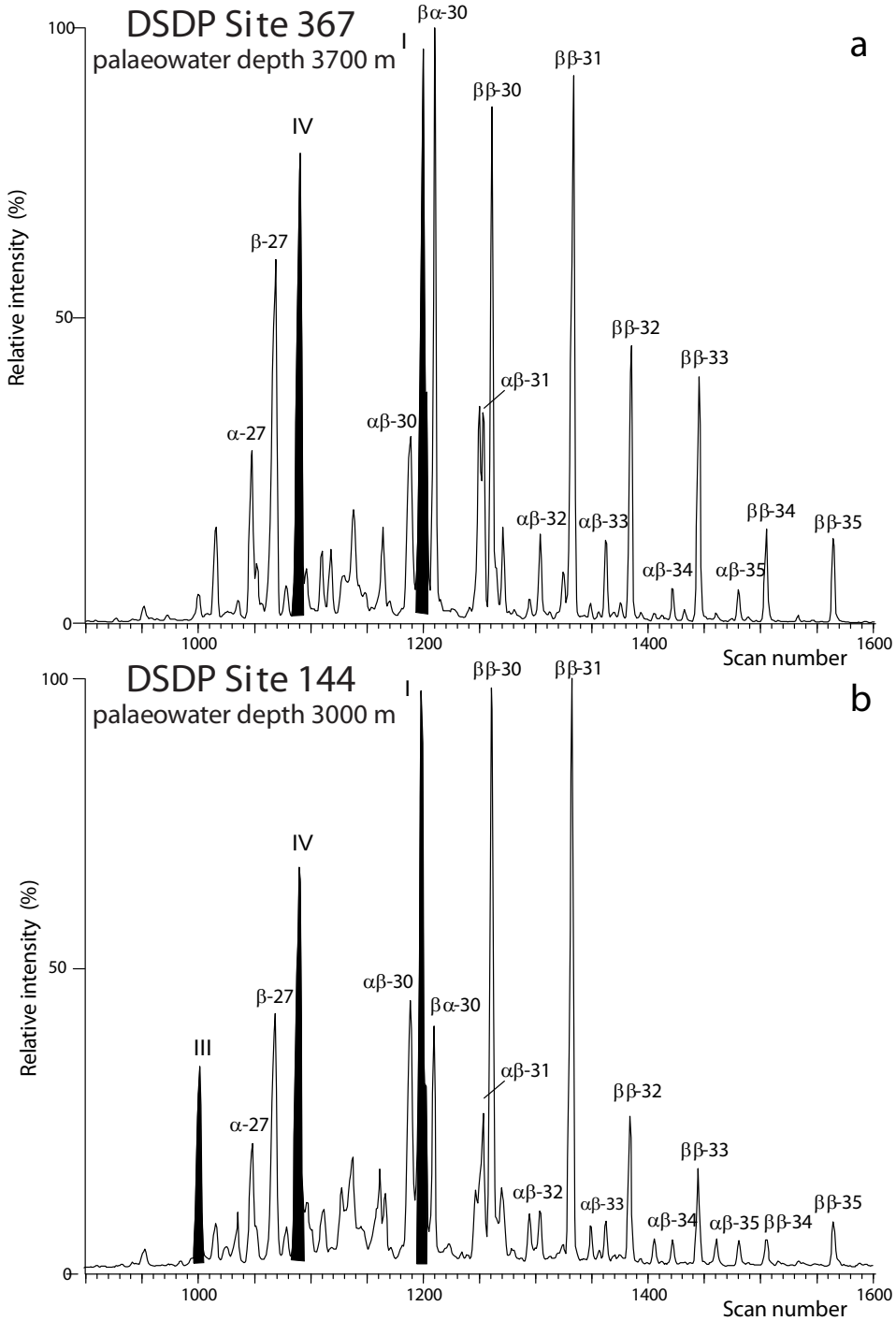

Fig. 3. Partial mass chromatograms of *m/z* 191 of the saturated hydrocarbon fraction (obtained by Ag^{+}-TLC) of Cenomanian black shales from the southern proto North Atlantic Ocean from (**a**) DSDP Site 367 (12°29.20'N 20°02.08'W, palaeowater depth 3700 m; 41-367-18-2 88-91 cm, 638.38 mbsf) and (**b**) DSDP Site 144 (09°27.23'N 54°20.52'W, palaeowater depth 3000 m; 14-144-04-2 0-30 cm, 214.60 mbsf). Peaks representing neo-13(18)-hopenes are black and hopanes are indicated by a shorthand notation indicating the stereochemistry at the C-17 and C-21 positions and total number of carbon atoms.

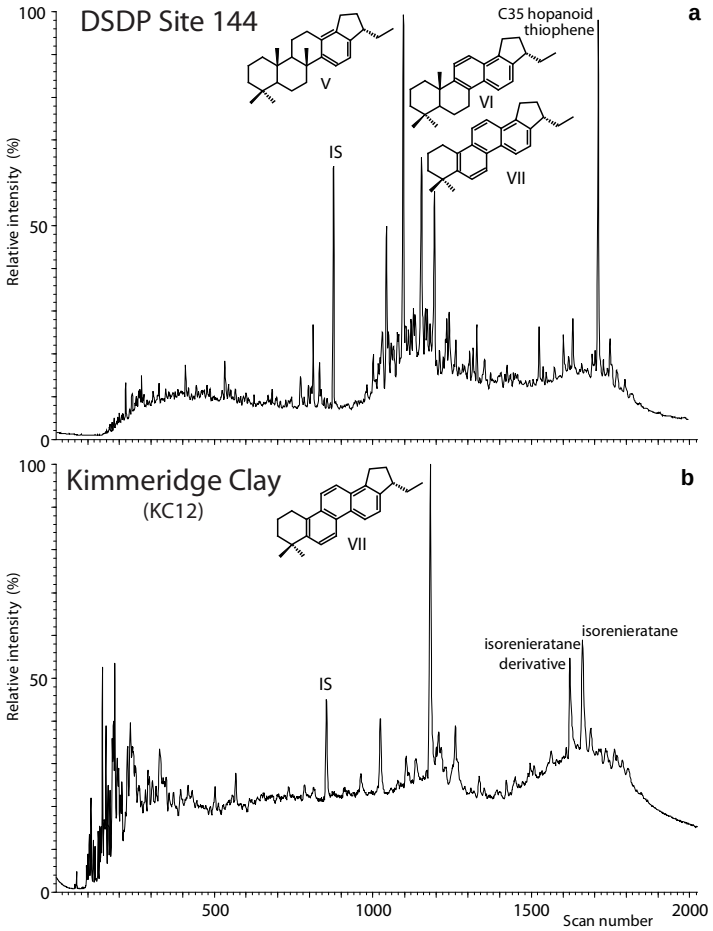

Fig. 4. Total ion current (TIC) trace of the aromatic hydrocarbon fractions of extracts of (**a**) a Cenomanian black shale from DSDP Site 144 (09°27.23'N 54°20.52'W, palaeowater depth 3000 m; 14-144-04-2 0-30 cm, 214.60 mbsf) and (**b**) a calcareous mudstone (D12; van Kaam-Peters et al., 1998) of the Kimmeridge Clay Formation outcropping at the coast of Dorset (UK). IS denotes internal standard.

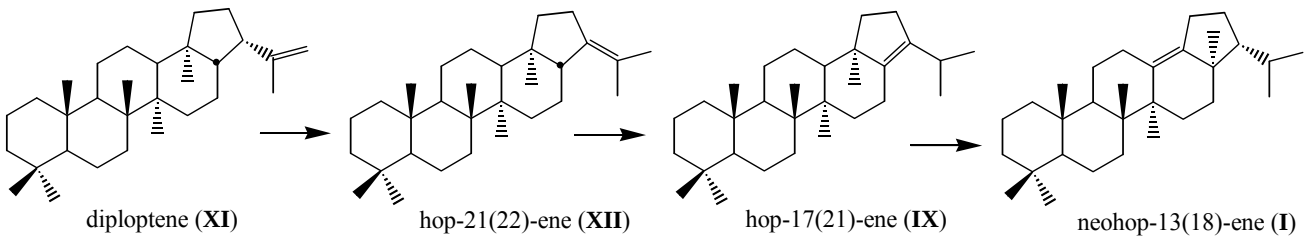

Fig. 5. Scheme showing the proposed isomerisation of diploptene (**XI**) to neohop-13(18)-ene (**I**) (after Ensminger, 1977).

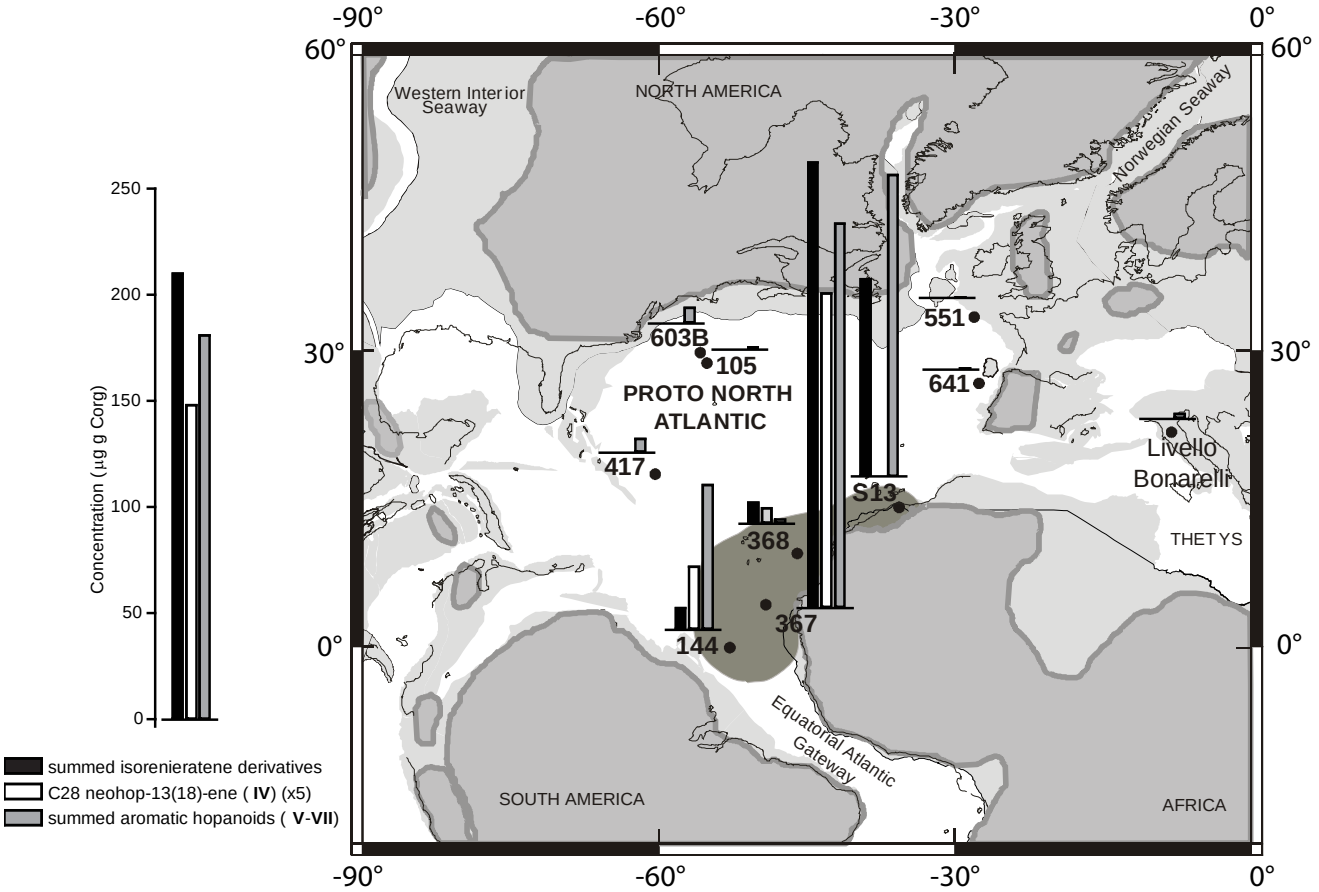

Fig. 6. Palaeogeographical map of mid Cretaceous (~93 My) North Atlantic showing the position of the Cenomanian black shales studied and concentrations of selected biomarkers as bar plots. Light grey regions represent continental plates (from GEOMAR map generator; www.odsn.de/odsn/services/paleomap/paleomap.html). Dark grey shaded regions represent land (Scotese and Golonka, 1992). The concentration of summed isorenieratene derivatives (black bars) is from Sinninghe Damsté and Köster (1998); they only occur in the dark grey coloured area between the South American and African continental plates characterized by photic zone euxinia. The concentration data of the C_{28} 28,30-dinorhop-13(18)-ene (**IV**; white bars) and the summed aromatic hopanoids (**V-VII**; grey bars) are from Table 1. For site S13 (Tarfaya, Morocco) the average values of the three samples in Table 1 are used. Note that the concentrations of the hopanoids **IV-VII** are 1-3 orders of magnitude higher in the area characterized by photic zone euxinia. All biomarkers concentrations are normalized on C_{org}.

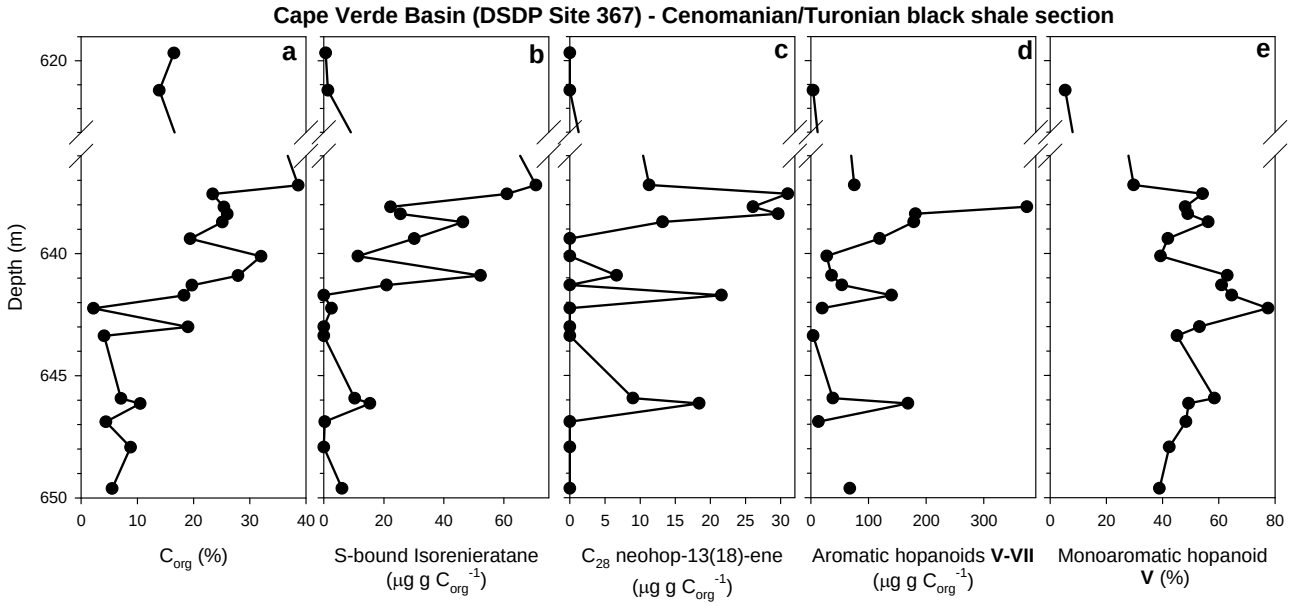

Fig. 7. Biomarker data for a Cenomanian/Turonian (OAE-2) black shale section from DSDP Site 367 (12°29.20'N 20°02.08'W, palaeowater depth 3700 m) in the southern proto North Atlantic Ocean. (**a**) C_{org} content (%) and concentrations of (**b**) isorenieratane released from the desulfurized polar fraction (see Kuypers et al., 2002 for details), (**c**) the C_{28} 28,30-dinorhop-13(18)-ene (**IV**), (**d**) the summed aromatic hopanoids (**V-VII**), and (**e**) the relative abundance of the monoaromatic hopanoid **V** relative to the sum of **V-VII**.

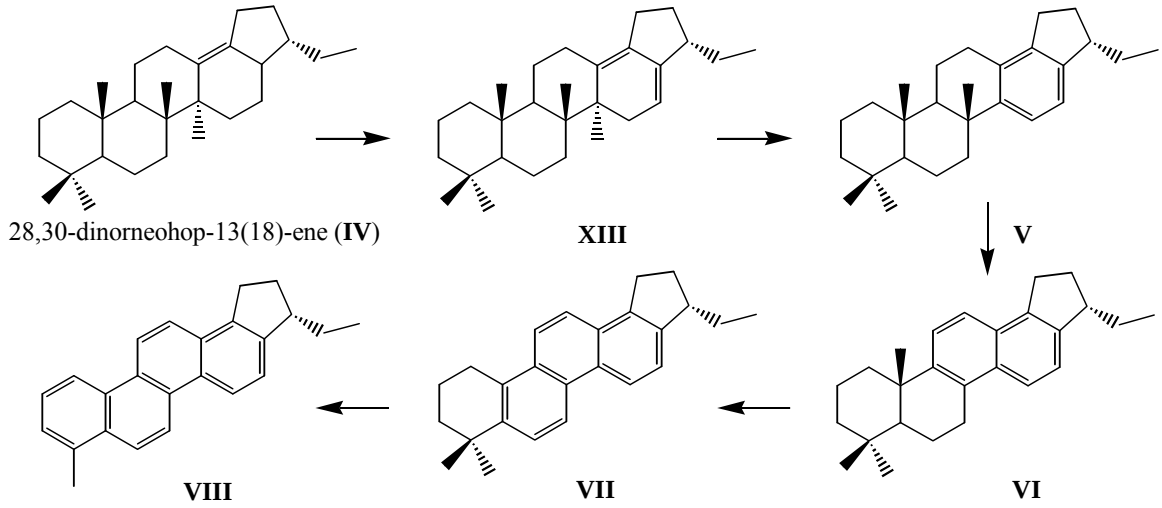

Fig. 8. Diagenetic scheme showing the possible formation of aromatic hopanoids **V-VIII** from the C_{28} 28,30-dinorhop-13(18)-ene (**IV**) through aromatisation starting in ring D (modified from Greiner et al., 1976, 1977). The tentatively identified intermediate **XII** was identified in a black shale from the Demerara Rise (DSDP Site 144).

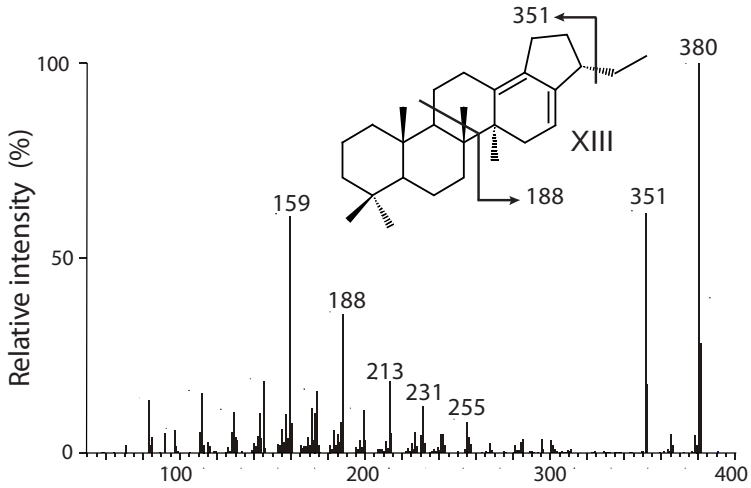

Fig. 9. Mass spectrum (background-subtracted) of 28,30-dinorhop-13(18),16-diene (**XIII**) tentatively identified in a black shale from Demerara Rise (09°27.23'N 54°20.52'W, DSDP Site 144; 14-144-04-2 0-30 cm, 214.60 mbsf). **XIII** is a potential intermediate in the conversion of the C_{28} 28,30-dinorhop-13(18)-ene (**IV**) into the aromatic hopanoids **V-VIII** (see Fig. 8).

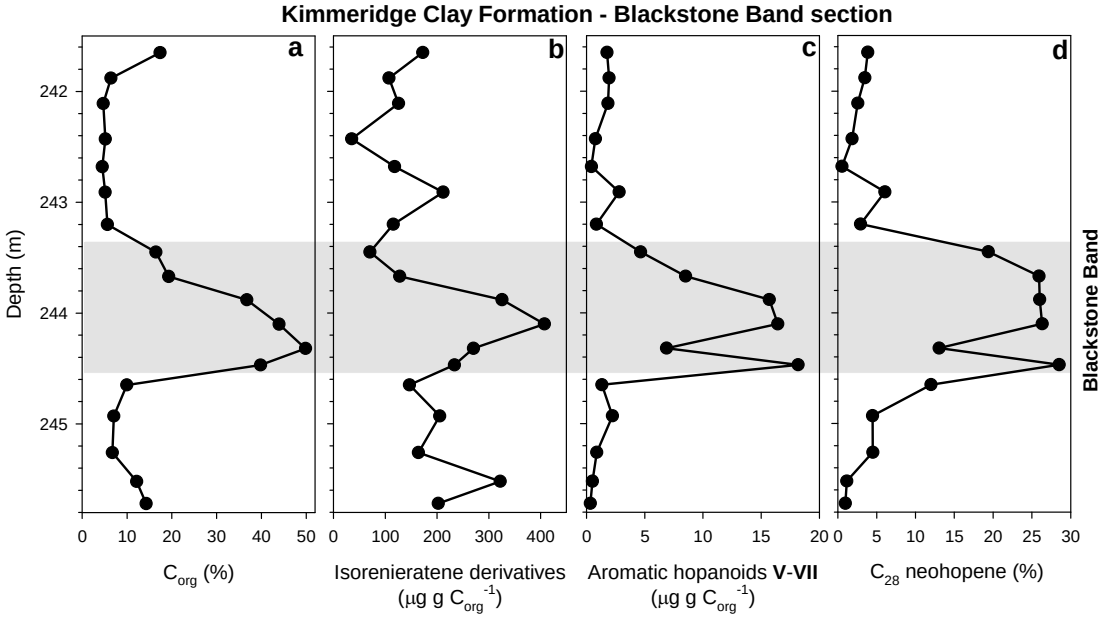

Fig. 10. Biomarker data for the Blackstone Band section of the Jurassic Kimmeridge Clay from the Swanworth Quarry 1 borehole [SY 9675 7823], South Dorset, UK. (**a**) C_{org} content (%) and concentrations of (**b**) isorenieratene derivatives (see van Dongen et al., 2006a for details), (**c**) the summed aromatic hopanoids (**V-VII**), and (**d**) the calculated relative abundance of the C_{28} 28,30-dinorhopene relative to total neohopenes. A complete description of the core is given by Morgans-Bell et al. (2001).

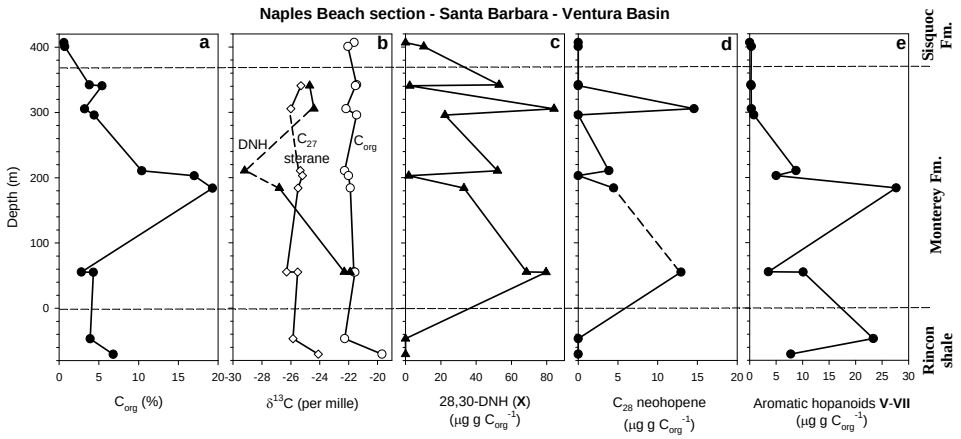

Fig. 11. Biomarker data for Miocene (ca. 6-19 Ma) black shales from the Naples Beach outcrop section of the Santa Barbara-Ventura Basin (California, USA). The depth is relative to the bentonite bed at the base of the Monterey Formation (see Isaacs et al, 2000). (**a**) C_{org} content (%) profile (from Schouten et al., 2002a) of the sediments used for biomarker investigations. (**b**) $\delta^{13}C_{org}$ (‰) (open circles), C_{27} sterane (open diamonds; composite record of free and sulfur-bound 5α-cholestane), and 17α,18α,21β(H)-28,30-DNH (closed triangles) (data from Schouten et al., 2002a). Concentrations of (**c)** 17α,18α,21β(H)-28,30-DNH (**d)** C_{28} 28,30-dinorhop-13(18)-ene, and (**e**) summed aromatic hopanoids. A stippled line indicates missing data points.

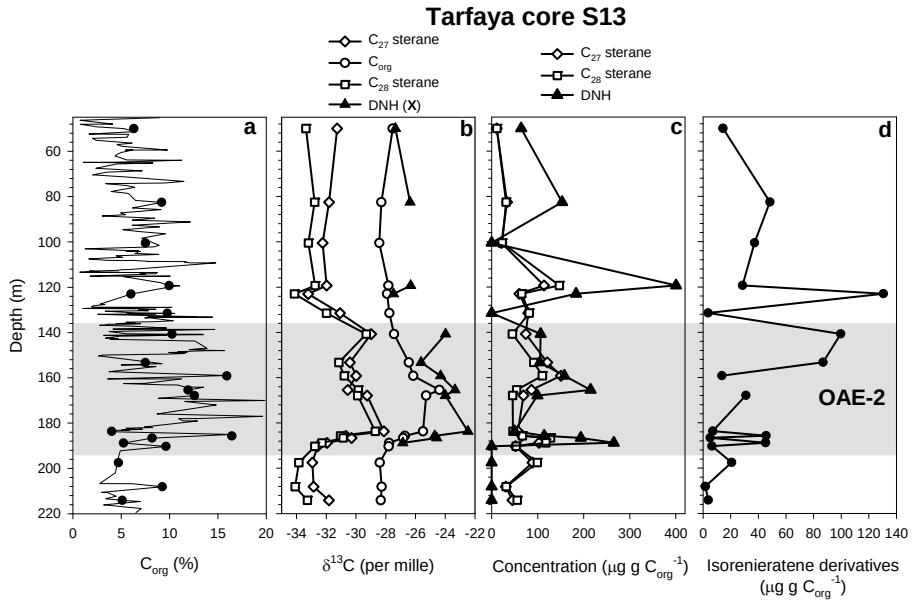

Fig. 12. Biomarker data for Cenomanian/Turonian (OAE-2) black shales from borehole S13 in the Tarfaya Atlantic Coastal Basin (Morocco). (**a**) High resolution C_{org} content (%) profile (from Kuhnt et al., 1997) and C_{org} content (black dots; Kuypers et al., 2002) of the sediments used for biomarker investigations. (**b**) $\delta^{13}C$ values (‰) of C_{org} and C_{27} (5α-cholestane) and C_{28} (24-methyl-5α-cholestane) steranes (data from Kuypers et al., 2002) and 17α,18α,21β(H)-28,30-DNH. (**c**) Concentrations of C_{27} and C_{28} steranes and 17α,18α,21β(H)-28,30-DNH. (**d)** Concentrations of isorenieratene derivatives (data from Kuypers et al., 2002). This represents the summed concentrations of sulfur-bound isorenieratene and isorenieratene derivatives in the aromatic hydrocarbon fraction.

Appendix

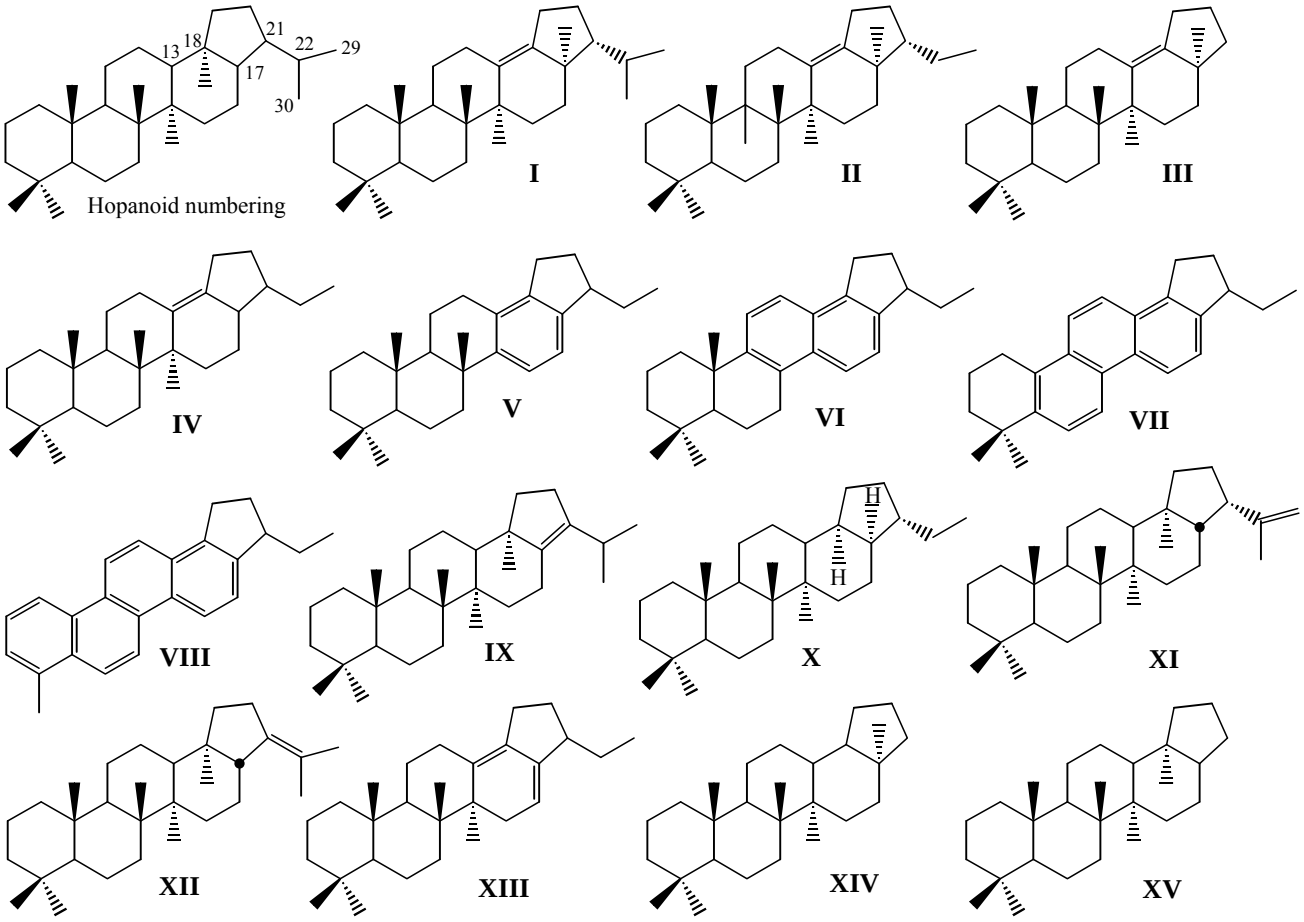
13
18
21
22
29
17
30
Hopanoid numbering
I
II
III
IV
V
VI
VII
VIII
IX
H
H
X
XI
XII
XIII
XIV
XV

Table 1: Concentration and distribution of hop-13(18)-enes and aromatic hopanoids in Cenomanian/Turonian black shales.

Sample	DSDP/ ODP Site	Location	Interval	Mbsf (m)	C_{org} (%)	17β,21β Hopane Isom.	Neohop-13(18)-enes **I-IV**					Aromatic hopanoids **V-VII**			
							Conc. (μg/g C_{org})	%C_{27}	%C_{28}	%C_{29}	%C_{30}	Conc. (μg/g C_{org})	%mono	%di	%tri
Lower Continental Rise Hill	105	34°53.72'N 69°10.40'W	11-105-9-3 123-128 cm	290.23	11.3	0.84	5.5	17	0	7	76	0.7	66	34	0
			11-105-9-4 74-80 cm	291.24	7.7	0.88	17	22	5	18	56	n.d.	n.a.	n.a	n.a
Demerara Rise	144	09°27.23'N 54°20.52'W	14-144-04-2 0-30 cm	214.60	6.8	0.75	15	19	40	0	41	68	44	35	21
Cape Verde Basin	367	12°29.20'N 20°02.08'W	41-367-17-3 68- 74 cm	619.68	16.5		1.3	17	0	0	83	n.a.	n.a.	n.a.	n.a.
			41-367-17-4 74- 80 cm	621.24	13.9		2.7	0	0	0	100	4.0	5	63	31
			41-367-18-1 120-124 cm	637.20	38.6		60	0	19	0	81	75	30	25	45
			41-367-18-2 6-9 cm	637.56	23.4		65	0	48	0	52	n.a.	54	22	24
			41-367-18-2 59- 62 cm	638.09	25.4		51	0	52	0	48	375	48	16	36
			41-367-18-2 88-91 cm	638.38	26.0	0.73	59	2	50	0	48	181	49	34	17
			41-367-18-2 121-125 cm	638.71	25.1		33	0	40	0	60	178	56	20	24
			41-367-18-3 39- 42 cm	639.39	19.4		15	0	0	0	100	119	42	11	47
			41-367-18-3 111-114 cm	640.11	32.0		6.3	0	0	0	100	28	39	27	34
			41-367-18-4 40- 43 cm	640.90	27.9		39	8	17	0	75	36	63	20	17
			41-367-18-4 79- 83 cm	641.29	19.7		9.9	0	0	0	100	54	61	14	25
			41-367-18-4 121-125 cm	641.71	18.3		76	6	28	0	66	140	65	13	22
			41-367-18-5 24- 30 cm	642.24	2.2		11	30	0	0	70	20	77	15	7
			41-367-18-5 100-106 cm	643.00	19.0		8.5	0	0	0	100	n.a.	53	14	33
			41-367-18-5 137-142 cm	643.37	4.1		5.4	33	0	0	67	4.1	45	15	40
			41-367-19-1 143-147 cm	645.93	7.1		28	10	32	0	58	38	58	33	9
			41-367-19-2 14-18 cm	646.14	10.5		36	9	51	0	39	168	49	14	37
			41-367-19-2 89- 94 cm	646.89	4.4		6.3	31	0	0	69	13	48	16	36
			41-367-19-3 43- 47 cm	647.93	8.8		6.5	0	0	0	100	n.a.	42	15	43
			41-367-19-4 62- 66 cm	649.62	5.5		0.0	n.a.	n.a.	n.a.	n.a.	68	39	18	43
	368	17°30.4'N 21°21.20'W	41-368-60-3 15-20 cm	952.65	6.4	0.85	22	10	7	7	77	2	22	44	34
			41-368-63-3 120-125 cm	979.20	11.9	0.00	0	n.a.	n.a.	n.a.	n.a.	56	0	27	73
Hatteras Abyssal	417	25°60.63'N 68°02.48'W	51B-417D-17-3 141-145 cm	300.71	5.8	0.87	0	n.a.	n.a.	n.a.	n.a.	6	18	62	20

Plain																
Goban Spur	551	48°54.64'N 13°30.09'W	80-551-05-2 69-75 cm	134.69	6.4	0.85	1.9	50	0	21	30	0.4	15	34	51
Lower Continental	603B	35°29.71'N 70°01.71'W	93B-603B-33-CC 4-7 cm	1122.91	8.4		11	19	0	23	57	2.6	0	83	17
			93B-603B-34-1 47-52 cm	1127.97	9.2		21	19	0	16	65	3.0	0	100	0
			93B-603B-34-1 101-105 cm	1128.51	5.9		30	15	0	18	67	6.9	0	100	0
			93B-603B-34-2 137-142 cm	1130.37	6.9		18	17	0	18	65	2.4	0	87	13
			93B-603B-34-3 65-70 cm	1131.15	7.4	0.84	36	22	0	17	61	7	0	68	32
			93B-603B-34-3 85-90 cm	1131.35	5.0		26	24	0	21	55	2.2	0	100	0
			93B-603B-34-3 114-120 cm	1131.64	1.3		10	13	0	27	60	0.0	n.a.	n.a.	n.a.
			93B-603B-34-4 12-18 cm	1132.12	0.2		0.9	7	0	20	73	9.4	0	100	0
			93B-603B-34-3 54-58 cm	1132.54	6.6		19	19	0	25	56	2.6	0	81	19
			93B-603B-34-5 4-10 cm	1133.54	2.6		41	14	0	30	57	7.7	0	83	17
			93B-603B-34-5 137-140 cm	1134.87	2.0		13	23	0	51	27	1.5	0	100	0
			93B-603B-35-3 81-86 cm	1140.31	2.3		10	15	0	45	40	2.4	0	96	4
Galicia Margin	641	42°09.30'N 12°10.90'W	103-641A-06X-CC	53.75	6.7	0.75	10	49	0	25	25	0.4	0	30	70
Tarfaya	n.a.		Core S13, 123 m	n.a.	5.7	0.13	15	11	0	10	79	57	55	32	13
			153 m	n.a.	7.5	0.09	20	8	0	40	52	104	36	25	40
			165 m	n.a.	11.0	0.09	20	6	0	57	37	264	22	14	64
Livello Bonarelli	n.a.		n.a.	n.a.	15.7	0.93	31	18	0	55	27	2	0	52	48

Table 2: Concentration and distribution of DNH, hop-13(18)-enes and aromatic hopanoids in Miocene black shales[a].

Sample	Depth[b]	Formation	C_{org}	DNH **X**	Neohop-13(18)-enes **I-IV**					Aromatic hopanoids **V-VII**			
	(m)		(%)	Conc. (μg/g C)	Conc. (μg/g C_{org})	$\%C_{27}$	$\%C_{28}$	$\%C_{29}$	$\%C_{30}$	Conc. (μg/g C_{org})	%mono	%di	%tri
KG-12	407	Sisquoc	0.6	0	19	21	0	0	79	0.0	n.a.[c]	n.a.	n.a.
KG-13	401	Sisquoc	0.7	10	3.9	0	0	0	100	0.3	0	0	100
KG-7	342	Monterey	3.8	53	12	16	0	0	84	0.2	0	0	100
KG-8	341	Monterey	5.4	2.4	4.4	100	0	0	0	0.3	0	0	100
KG-5	305	Monterey	3.2	84	34	9	43	0	48	0.3	0	0	100
KG-6	296	Monterey	4.4	22	10	40	0	0	60	0.8	0	0	100
KG-1	211	Monterey	10.4	52	15	21	25	0	54	8.7	51	15	35
KG-4	203	Monterey	17	1.8	14	34	0	0	66	5.0	25	15	60
KG-2	184	Monterey	19.3	33	18	22	25	0	53	28	47	10	43
KG-11	55	Monterey	2.8	68	n.d.[d]	n.d.	n.d.	n.d.	n.d.	3.5	79	21	0
KG-10	55	Monterey	4.3	80	31	29	42	0	29	10	34	9	56
KG-9	-47	Rincon Shale	3.9	0	30	29	0	0	71	23	46	19	36
KG-3	-70	Rincon Shale	6.8	0	19	12	0	0	88	7.8	20	14	65

[a] see Isaacs et al. (2000) for a general description of these rocks of the Santa Barbara-Ventura Basin outcropping at Naples Beach (California, USA)
[b] relative to the bentonite bed at the base of the Monterey Formation. (Isaacs et al, 2000)
[c] n.a. = not applicable
[d] n.d. = not determined

Table 3: Concentration and distribution of hop-13(18)-enes and aromatic hopanoids in Kimmeridgian black shales.

Sample	Depth	Pectinatites	Lithology	$C_{org.}$	Neohop-13(18)-enes **I-IV**					Aromatic hopanoids **V-VII**			
	(m)	biozone[a]		(%)	Conc. (µg/g C_{org})	$\%C_{27}$	$\%C_{28}$	$\%C_{29}$	$\%C_{30}$	Conc. (µg/g C_{org})	%mono	%di	%tri
Outcrop[b]													
D1	0	*pectinatus*	laminated coccolith-rich limestone	4.5	74	0	0	24	76	164	0	9	91
D2	19.3	*hudlestoni*	tabular cementstone	0.6	45	0	0	62	38	3	0	0	100
D3	42.4	*hudlestoni*	coccolith-rich limestone	7.0	55	0	0	36	64	83	0	10	90
D4	42.6	*hudlestoni*	oil shale	24.1	36	0	0	52	48	40	0	5	95
D5	43.7	*hudlestoni*	bituminous mudstone	18.2	80	0	0	45	55	42	0	14	86
D6	44.3	*hudlestoni*	mudstone, undifferentiated	6.2	66	0	0	55	45	44	0	9	91
D7	45.6	*hudlestoni*	coccolith-rich limestone	2.1	62	0	0	52	48	90	0	2	98
D8	45.9	*hudlestoni*	coccolith-rich limestone	10.7	69	0	0	37	63	214	0	2	98
D9	50.6	*wheatleyensis*	oil shale (Blackstone Band)	52.1	49	0	0	26	74	32	0	6	94
D10	51.4	*wheatleyensis*	bituminous mudstone	4.8	87	0	0	58	42	9	0	22	78
D11	53.2	*wheatleyensis*	oil shale	10.8	74	0	0	49	51	16	0	13	88
D12	53.7	*wheatleyensis*	calcareous mudstone	3.7	74	0	0	60	40	16	0	19	81
D13	57.2	*wheatleyensis*	calcareous mudstone	7.4	73	0	0	55	45	560	0	0	100
Core SY 9675 7823[c]													
KCF1	241.65	*wheatleyensis*		17.4	44	0	0	48	52	1.8	0	31	69
KCF2	241.88	*wheatleyensis*		6.4	54	0	0	58	42	1.9	0	21	79
KCF3	242.11	*wheatleyensis*		4.7	70	0	0	63	37	1.8	0	16	84
KCF4	242.43	*wheatleyensis*		5.2	40	0	0	68	32	0.8	0	20	80
KCF5	242.68	*wheatleyensis*		4.5	76	0	0	66	34	0.4	0	20	80
KCF6	242.91	*wheatleyensis*		5.1	43	0	0	42	58	2.8	0	24	76
KCF7	243.2	*wheatleyensis*		5.6	28	0	0	54	46	0.8	0	38	62
KCF8	243.45	*wheatleyensis*		16.4	19	0	0	57	43	4.6	0	7	94
KCF9	243.67	*wheatleyensis*		19.3	24	0	0	37	63	8.5	0	9	91
KCF10	243.88	*wheatleyensis*	oil shale (Blackstone Band)	36.8	45	0	0	44	56	15.7	0	10	90
KCF11	244.1	*wheatleyensis*	oil shale (Blackstone Band)	43.9	46	0	0	38	62	16.4	0	6	94
KCF12	244.32	*wheatleyensis*	oil shale (Blackstone Band)	49.9	46	0	0	42	58	6.9	0	1	88
KCF13	244.47	*wheatleyensis*	oil shale (Blackstone Band)	39.8	46	0	0	47	53	18.2	0	6	94
KCF14	244.65	*wheatleyensis*		9.9	10	0	0	61	39	1.3	0	10	89
KCF15	244.93	*wheatleyensis*		7.1	47	0	0	55	45	2.2	0	13	87

KCF16	245.26	*wheatleyensis*	6.7	18	0	0	79	21	0.9	0	37	63
KCF17	245.52	*wheatleyensis*	12.1	42	0	0	55	45	0.5	0	22	78
KCF18	245.72	*wheatleyensis*	14.3	32	0	0	54	46	0.3	0	47	53

[a] according to Cox and Gallois (1981)
[b] data from van Kaam-Peters et al. (1998)
[c] data from van Dongen et al. (2006a); detail on core in Morgan-Bells et al. (2001)

Table 4: Characteristic mass spectral fragment ions of C_{27}-C_{30} neohop-13(18)-enes

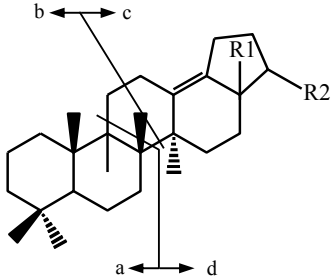

Neohopene	Mass spectral ion (*m/z*)					
	$M^{+\bullet}$	Fragment a	Fragment b	Fragment c $C_{12+n}H_{19+2n}$	Fragment d $C_{13+n}H_{20+2n}$	Fragment e $C_{14+n}H_{21+2n}$
C_{27} (**III**; n=0)	368	191	205	163	176	187
C_{28} (**IV**; n=1)	382	191	205	177	190	201
C_{29} (**II**; n=2)	396	191	205	191	204	215
C_{30} (**I**; n=3)	410	191	205	205	218	229

Table 5: $\delta^{13}C$ (‰) values[a] for neohop-13(18)-ene and related compounds identified in this study.

Biomarker	Origin					
	Arabian Sea[b] (NIOP 451)	Monterey[c] (SB-1)	Monterey[d] (KG1)	Monterey[d] (KG10)	Cape Verde Basin[e] (DSDP 367)	Demerara Rise[e] (DSDP 144)
C_{27} Neo-hop-13(18)-ene (**III**)	n.d.[f]	-26.0±0.2			n.d.	-26.7
C_{28} 28,30-Dinorhop-13(18)-ene (**IV**)	n.a.[g]	n.a.			-16.6	-26.5
C_{30} Neohop-13(18)-ene (**I**)	-20.7±1.3	-22.2±0.2			-22.6	n.d.
Hop-17(21)-ene (**IX**)	-24.2±0.4	-27.8±0.5			-20.8	n.d.
Monoaromatic hopanoid (**V**)	n.d.	n.d.			-16.6±0.2	-25.9±0.1
Diaromatic hopanoid (**VI**)	n.d.	n.d.			-15.9±0.1	-25.8±0.2
Triaromatic hopanoid (**VII**)			-22.9±0.4	-21.6±0.6		
17α,18α,21β(H)-28,30-DNH (**X**)	n.a.		-29.2±0.2	-21.9±0.3	n.a.	n.a.
Trinorhopane	n.a.		-30.8±0.2	-22.7±0.6	n.a.	n.a.
C_{25} HBI	-23.2	-27.6	-22.0±0.5	n.d.	n.a.	n.a.
C_{30} HBI	-26.7		n.a.	n.a.	n.a.	n.a.
Lycopane	-23.5	-25.4±0.3	-27.5±1.5	-32.6±1.0	n.d.	-28.0
Isorenieratane[h]	n.a.	n.a.	n.a.	n.a.	-13.5±0.3	-17.7±1.2
C_{35} hopane[h]			-29.5±0.8	-27.0±0.8	-22.7±0.3	-29.4±0.6
Phytane[h]		-26.3±0.2	-25.4±0.4	-23.4±0.1	-24.4±0.3	-31.0±0.4

[a] where appropriate errors indicate the standard deviation from 2-4 measurements; large errors typically indicate high background.
[b] all data except for hopenes reported by Schouten et al. (2000b)
[c] all data except for hopenes reported by Schouten et al. (1997)
[d] all data except for triaromatic hopanoid reported by Schouten et al. (2000c)
[e] all data except for hopenes and aromatic hopanoid reported by Sinninghe Damsté and Köster (1998) and Sinninghe Damsté et al. (2008)
[f] n.d.=not determined because of low concentration or co-elution with another component
[g] n.a. = not applicable, i.e. component is not present
[h] released by desulfurisation of polar fraction

Table 6: Concentration of aromatic hopanoids **V-VII** and their distribution in an organic-rich limestone from the Ghareb Formation and in rocks artificially matured at temperatures in the range 200-300°C using hydrous pyrolysis[a].

	Concentration (μg/g TOC)	V	VI (%)	VII
Original	33	65	35	0
200°C	222	20	8	72
220°C	217	24	8	68
240°C	234	22	9	70
260°C	237	23	17	60
280°C	103	42	17	40
300°C	46	0	0	100

[a] Details of the experiments can be found in Koopmans et al. (1998)

Table 7: $\delta^{13}C$ (‰) values[a] and concentrations of 20R 5α,14α, 17α(H)-steranes and 17α,18α,21β(H)-28,30-DNH in Cenomanian/Turonian black shales from the Tarfaya Basin (core S13)[b].

depth	C_{org}	$\delta^{13}C$ (‰)				Concentration (μg g C_{org}^{-1})			
(m)	(%)	C_{org}	C_{27} sterane	C_{28} sterane	DNH	C_{27} sterane	C_{28} sterane	DNH	Isorenieratene derivatives
50.0	6.3	-27.5	-31.3±0.5	-33.4±0.2	-27.4±0.1	11	11	64	14
82.5	9.2	-28.3	-31.8±0.2	-32.8±0.2	-26.4±0.1	33	31	153	48
100.5	7.5	-28.4	-32.2±0.3	-33.2±0.2	n.a.[b]	21	23	0	37
119.3	10.0	-27.8	-32.0±0.1	-32.8±0.2	-26.3±0.2	114	147	401	29
123.0	6.0	-27.9	-33.2±1.5	-34.1±0.7	-27.5±0.1	60	65	183	131
131.5	9.8	-27.8	-31.1±0.6	-32.0±0.8	n.a.	79	81	0	3.7
140.7	10.3	-27.4	-29.0±0.3	-29.3±1.0	-24.0±0.4	74	45	106	100
153.3	7.5	-26.4	-30.4±0.9	-31.2±0.3	-25.6±0.6	121	91	105	87
159.2	15.9	-26.2	-30.0±0.1	-30.8±0.2	-24.3±0.2	150	110	158	14
165.4	11.9	-24.4	-30.6±1.3	-29.9±0.5	-23.3±0.5	86	54	215	n.d.[c]
167.9	12.6	-25.3	-29.3±0.4	-29.9±0.1	-24.0±0.1	69	45	99	31
183.7	4.0	-25.5	-28.1±0.7	-28.7±0.7	-22.5±0.5	57	46	49	7.1
185.7	16.4	-26.7	-30.7±0.2	-31.0±0.1	-24.7±0.1	66	66	114	46
186.6	8.2	-26.8	-30.3±0.2	-30.9±0.3	-24.6±0.1	117	128	194	5.1
188.8	5.2	-27.8	-31.9±0.4	-32.3±0.1	-26.9±0.1	103	118	265	45
190.3	9.6	-27.8	-32.6±1.2	-32.8±0.7	n.a.	51	53	0	6.5
197.5	4.7	-28.4	-32.9±0.6	-33.8±0.9	n.a.	88	99	0	21
208.1	9.2	-28.3	-32.9±0.5	-34.1±0.2	n.a.	31	31	0	1.6
214.1	5.1	-28.3	-31.8±0.2	-33.3±0.3	n.a.	45	55	0	3.7

[a] errors indicate the standard deviation from 2 measurements; large errors typically indicate high background.
[b] background data, isotopic composition of steranes, and concentration of isorenieratene derivatives previously reported by Kuypers et al. (2002).
[c] n.a. = not applicable
[d] n.d. = not determined